Davie and Ausió *Epigenetics & Chromatin* (2026) 19:23
https://doi.org/10.1186/s13072-026-00671-4

Epigenetics & Chromatin

REVIEW Open Access

From chromosomal protein disorder to chromatin phase separation

James R. Davie[1] and Juan Ausió[2*]

Abstract

In recent years, two seemingly unrelated topics, protein disorder and phase separation, have become highly significant in biology. In this way, intrinsically disordered proteins and liquid-liquid phase separation have become two of the hottest topics in the field. In this review, we provide a brief description of intrinsic protein disorder and its effects on the main protein constituents of chromatin, from histones to high-mobility group proteins, heterochromatin HP1, the neuronal methyl-CpG binding protein 2, and the highly specialized arginine-rich protamines of sperm. Following this, we provide a general overview of the role of their intrinsically disordered regions (IDRs) in chromatin condensate formation and present the evolving understanding of the amino acid sequence grammar of IDRs that determines their involvement in in the formation of chromatin condensates. After a brief overview of the theoretical aspects beyond this process, we describe how it is connected to the folding of somatic and male germ cell chromatin. Somatic cell chromatin is organized into compartments. We discuss the characteristics of the phase-separated transcription condensate in compartment A (euchromatin), including the specialized biomolecular condensate in which replication-dependent histone genes are transcribed, and the differential structure and role of HP1 alpha in compartment B heterochromatin compaction across different species.

Highlights

- Protein disorder plays an important role in the LLPS-mediated formation of chromatin condensates.
- Alterations of intrinsically disordered regions of proteins have important disease implications and targeting IDP/IDRs with de novo binders may have important therapeutic implications.
- Liquid-liquid phase separation is involved in the compartmentalization of both nucleosome - organized chromatin and protamine-organized sperm chromatin.
- Liquid-liquid phase separation has a critical role in driving the condensate formation.

Keywords Intrinsically disordered proteins, Chromatin, Liquid-liquid phase separation

*Correspondence:
Juan Ausió
jausio@uvic.ca
[1]Department of Biochemistry and Medical Genetics, Max Rady College of Medicine, University of Manitoba, Winnipeg MB R3E 0J9, Canada
[2]Department of Biochemistry and Microbiology, University of Victoria, Victoria, BC V8W 2Y2, Canada

Introduction

With approximately 40% of the protein residues located in intrinsically disordered regions (IDRs) in proteins [1, 2], intrinsic disorder represents one of the most prevalent secondary structure features of proteins. In contrast to the unidirectional "lock-and-key" structure-to-function paradigm that has pervaded biochemistry textbooks in the past, IDRs enable greater functional multiplicity by interacting with a wide range of partners, including DNA, RNA, and proteins. It is through these kinds of interactions that they can participate in the formation of membrane-less structural condensates [1], which are responsible for functional compartmentalization within the cell [2]. The condensate formation often involves liquid-liquid or solid-like phase separation (LLPS/SLPS) (see below) [3], a process with health implications [4]. In this review, we will focus on the intrinsic properties of chromosomal proteins and their ability to form biologically relevant nuclear condensates, particularly as they pertain to chromatin.

Intrinsically disordered proteins (IDPs)

The discovery of the important role of disorder in proteins [5–8] represented an important cornerstone in the field of protein chemistry [9]. By that time, in 2001, in a paper published with Keith Dunker on IDPs, we proposed the Protein Trinity concept, which suggests that the native protein structure can encompass not only ordered states but also random coil and molten globule states, and that function may depend on any of these states or transitions between them [6]. Despite the lack of a fixed secondary or tertiary structure, many regions within IDPs and within intrinsically disordered regions (IDRs) of multi-domain proteins can adopt defined secondary structures and an ordered three-dimensional organization upon interaction with their binding partners (DNA, RNA, or other proteins) [10]. Although the fundamental role of intrinsic protein disorder is now widely recognized, it took some time to be incorporated into textbooks [9] and to gain the mainstream acceptance it has today.

IDR and biomolecular condensates

IDRs are regions in proteins that lack a fixed secondary and tertiary structure (1, 11). They encompass dynamic polypeptide regions that are often low in bulky hydrophobic amino acids, with a prominent presence of glycine and proline helix breakers [11] and are often enriched in polar and charged amino acids such as glutamic, lysine and arginine [12]. IDRs usually refer to short polypeptide stretches interspersed between other structurally organized domains of a protein (Fig. 1), whereas IDPs relate to proteins with an entirely disordered sequence. While this last type of protein is relatively rare, Fig. 1C-E provide good examples of this definition.

Nuclear proteins (e.g., histones, RNA polymerase II) are enriched in IDRs [1, 13]. Nuclear IDR-containing proteins play a crucial role in the formation of biomolecular condensates and the organization and function of the nucleus and chromatin [14, 15]. Highlighting the importance of the IDR are studies demonstrating that the mutation or loss of an IDR results in human disease [16, 17] .

Biomolecular condensates, which lack membranes and are numerous in the interphase nucleus, have specific functions. These are formed by weak, multivalent, noncovalent interactions between proteins with similar functions [18, 19]. These weak interactions include Pi-Pi interactions between aromatic (Phe, Tyr, Trp, His) and non-aromatic (Gln, Asn, Glu, Asp and Arg) amino acids [20, 21], ionic bonds, and hydrogen bonds. Examples of nuclear biomolecular condensates include nuclear bodies (such as the nucleolus, nuclear speckles, and promyelocytic leukemia nuclear bodies), transcriptional condensates, and heterochromatin [22–25].

Recent studies have identified the features of a protein sequence that direct the protein to a specific nuclear condensate. Machine learning [18, 26] (ProtGPS) and high-throughput pooled imaging with in situ sequencing [27] (CondenSeq) approaches have shed light on the condensate-targeting sequences.

IDR grammar

The amino acid sequence of the IDR has a grammar or code that determines the properties of the IDR-containing protein, including its recruitment to specific condensates, nuclear location, and cellular function [13, 15, 19, 28, 29]. A protein's IDR can adopt a range of conformations and functions, which may be cell-dependent and multifaceted depending on the protein's interactome. Not all IDRs will be involved in biomolecular condensate formation and serve roles, for example, in protein-protein interactions or chromatin binding. Understanding the IDR code is an ongoing and essential research question [9, 30]. IDRs that promote phase separation are often rich in polar, charged residues (Arg, Lys, Asp, Glu) and aromatic amino acids (Phe, Tyr). The pattern of a sequence or aromatic amino acid in an IDR is also involved in phase-separated biomolecular condensates. In Shi et al.'s review [30], they identified three types of amino acids/peptides in IDRs engaged in the formation of phase-separated biomolecular condensates: amino acid stickers (e.g. aromatic residues); short linear motifs that are involved in weak multivalent interactions as a set of fixed residues; and spacers which separate stickers, short linear motifs or structural domains [30].

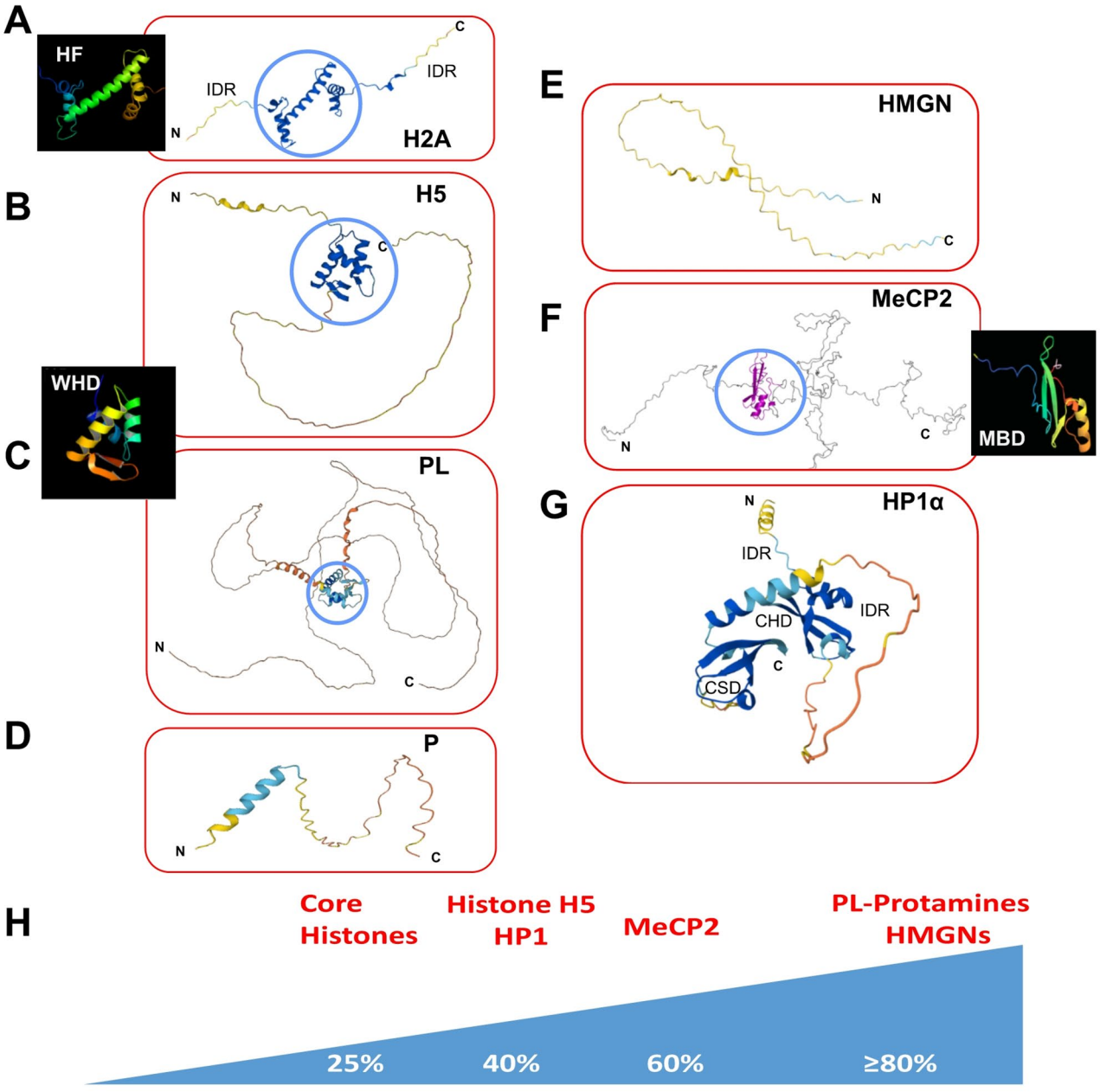

1 Davie and Ausió 2025

Fig. 1 Intrinsic disorder of chromatin proteins. **A** core histone H2A, **B** chicken erythrocyte linker histone H5, **C** protamine-like (PL) protein from the surf clam *S. solidissima*, **D***Loligo opalescens* squid protamine (P), **E** human HMGN1, **F** human MeCP2, **G** human HP1α. The three-dimensional organization of the winged helix domain (WHD), histone fold (HF), methyl binding domain (MBD), chromodomain CHD) and chromoshadow domain (CSD) are also shown. The images **A**-**D** and **E** and **G** were produced with the help of AlphaFold Protein Structure Database (see list of is references) and the image in F was obtained using a combination of all-atom and coarse-grained simulations. **H** Graphic representation of the extent of protein disorder. IDR: intrinsically disordered region; C: C-termini and N: N-termini

Martin et al. identified the sequence features that determined how intrinsically disordered prion-like domains (PLD) promote liquid-liquid phase separation [31]. The authors proposed a sticker (aromatic residues) and spacer lattice model. They demonstrated that the number and spacing of aromatic residues (stickers) were important sequence features of the PLD. The nonrandom, uniform distribution of aromatic residues was observed in IDRs of FUS, TAF15, EWSR1, hnRNPA2B1, hnRNPA3, POLR2A, SUPT5H, DHX9, and GAR1. Naderi J et al. [32] analyzed 1,500 transcription factors and identified 531 with an IDR containing at least one block of four

aromatic amino acids. These transcription factors IDRs were enriched in aromatic residues ("Stickers") and serines ("spacers") and depleted in charged amino acids. Most of these IDRs were distinct from the transcription factor's activation domain. The arrangements of these aromatic residues were important to the transcriptional activity of the transcription factor. Interestingly, the study showed that the arrangement and number of aromatic repeats were suboptimal for transcriptional activity and could be improved. However, the factor's DNA-binding specificity was compromised. Tests with the HOXD4 IDR demonstrated that the dispersion of aromatic amino acids was suboptimal. Increasing the periodicity by substituting non-aromatic with Y improved transactivation activity but also altered gene specificity. Decreased heterodimerization and increased RNAP II interaction may contribute to changes in gene specificity. Studies with other transcription factor IDRs (HOXC4, OCT4, PDX1, FOXA3, C/EBPα) demonstrated that increased aromatic dispersion increased transcriptional activation. Optimizing the dispersion of aromatic residues enhanced transcription-factor-driven reprogramming (e.g., C/EBPα and macrophage reprogramming; MYOD1 and myotube differentiation; NGN2 and neural differentiation). The authors discuss that having a suboptimal dispersion of aromatic residues in a transcription factor is the price to pay for gains in specificity in transcriptional control.

Patil et al. applied the NARDINI+ algorithm to analyze the IDRs of the subunits of the mammalian SWI/SNF family of chromatin remodelers [13]. The NARDINI+ algorithm combines the NARDINI algorithm with FAIDR. The NARDINI (Non-random Arrangement of Residues in Disordered Regions Inferred using Numerical Intermixing) algorithm was developed to identify significant binary patterns with IDRs [33]. A statistical model named FAIDR (Feature Analysis of Intrinsically Disordered Regions) was generated to exploit sequence-distributed molecular features (repeats, biophysical properties, short linear motifs) to predict the function of an IDR and associate the molecular feature(s) of the IDR with a biological function [34].

Recently, Ruff and coauthors reported a resource called Grammars Inferred using NARDINI+ (GIN) to classify IDRs into 30 clusters, created by analyzing 24,508 human IDRs [35]. As examples, long D/E tracks (cluster 7), patches of R (cluster 26), and A patches (cluster 20). The protein IDRs within a specific cluster were present in distinct subcellular locations. For example, blocks of Ks (cluster 23), long D/E tracks (cluster 7), and large blocks of negatively and positively charged amino acids (cluster 18) were enriched in the nucleoli, while IDRs with patches of R (cluster 26) were enriched in nuclear speckles (also known as interchromatin granule clusters). The authors note that the specific grammar of the IDRs is insufficient to direct proteins to particular locations. Specific biological functions were enriched in an IDR cluster. Transcription regulation was enriched in Q tracts (cluster 11 IDRs), and chromatin organization was enriched in large blocks of negatively and positively charged amino acids (cluster 18 IDRs).

Adding to the complexity of the IDR grammar are post-translational modifications (PTMs). IDR PTMs can alter charge or hydrophobicity, thereby changing the properties of the IDR, its structure, and its interactome [36–38]. For examples, the IDRs of MED1 and lysine acetyltransferase 3 A/B (KAT3A/B) undergo acetylation, which alters the properties of the proteins and their interactome in the condensate [39, 40]. In the case of chromatin, global IDR N-terminal acetylation of histones alters the compaction of the chromatin nucleofilament, and its ability to aggregate [41], and phosphorylation of protamines modulates the efficiency of DNA condensation [42].

De La Cruz and coauthors demonstrated that swapping IDRs of the MED1 and FUS proteins redirected the proteins to different condensates and established a specific protein interactome in that condensate [19]. MED1 is a subunit of a multiprotein complex named Mediator, which plays a critical role in the transcription of genes. FUS is an RNA-binding protein also involved in transcription and RNA splicing. The FUS IDR1 is rich in Q, S, G and Y, while the MED1 IDR is rich in positively and negatively charged amino acids.

IDRs and disease

Nonsense and frameshift mutations of IDRs (e.g., KAT3A's cluster 11 IDR) are present in cancer-driving genes, including fusion oncogenes [43]. The mutation in a protein's IDR could potentially alter the protein's modification states, nuclear localization, ability to form or dissolve condensates, and/or alter the protein's interactome (protein-protein, protein-DNA, protein-chromatin, protein-RNA). The KMT2A-MLLT3 fusion oncoprotein is frequently found in acute myeloid leukemia and is a driver of this cancer. In the fusion protein, KMT2A retains the IDRs in the N-terminal part of the protein but has lost multiple IDRs in the protein's C-terminus, while in MLLT3, several of the fusion events result in the truncation of MLLT3's IDR. Together, these alterations in the IDRs will impact condensate formation and protein interactions. MLLT3 is a member of the YEATS family, which are readers of acetylated and crotonylated lysines. The MLLT3 IDR is located in its C-terminal part. Disorder to ordered folding occurs when the IDR binds to partner proteins (AF4, KMT4, BCOR, CBX8) [44].

The altered grammar/code of HMGB1's IDR targeting the frameshift mutant to the nucleolus, resulting in disruption of the nucleolar structure and function and cell

death [16]. The frameshift mutation resulted in the grammar of the HMGB1's C-terminal tail IDR from an acidic E/D rich sequence to a K/R rich basic sequence with a hydrophobic patch at the C-terminus of this sequence. The frameshift is proposed to be the mechanism underlying the rare genetic diseases brachyphalangy, polydactyly, and tibial aplasia/hypoplasia syndrome.

Highly disordered structural chromatin proteins

IDPs are overrepresented in the nucleus [45] and chromosomal proteins provide one of the best examples. This is no surprise, as their disordered organization allows these proteins to interact with a plethora of different binding partners within the nucleus.

In this review, we will focus our attention on some of the most abundant structural chromatin proteins [46] whose commonality is the presence of IDRs, leading to varying degrees of protein disorder (Fig. 1H).

Histones

Histones are amongst one of the most abundant chromosomal proteins and are responsible for the architectural organization of chromatin [47]. They are rich in arginine and lysine, and range in mass from 10 to 25 kDa. They can be classified into two main groups: core histones and linker histones. The former are responsible for organizing DNA into nucleosomes (the basic subunit of chromatin), and the latter bind to the linker DNA connecting them [47]. Core histones H2A and H2B consist of a folded histone fold (HF) [48] flanked by N-terminal and C-terminal IDRs [49, 50] (Fig. 1A), whereas histone H3 and H4 lack the C-terminal IDR. Linker histones (histone H1 family) consist of a central winged helix fold domain (WHD) [51] as in histone H5 [52] (Fig. 1B), and their N- and C-terminal ends are also intrinsically disordered. The structures shown in Fig. 1 were obtained from the AlphaFold Protein Structure Database [53, 54], except for F, which was determined using a combination of all-atom and coarse-grained simulations [55]. Core histone IDRs have been shown to be involved in LLPS, for instance, the N-terminal tail lysine residues of histone H4 have been shown to be the main drivers of LLPS of nucleosome arrays [56] and that nucleosomes can be brought together by histone H1 into phase-separated droplets [57, 58].

The core histones and H1 undergo a variety of PTMs, which are catalyzed by writers (enzymes that add the PTM) and removed by erasers (enzymes that remove the PTM). Readers are proteins/enzymes that bind to a specific modified site(s) on the histone. Together, the writers, readers, erasers, and histone PTMs establish a "histone code" [59]. Adding to the complexity of the histone, the five histones have variants that are the products of different genes [24]. Histone variants and PTMs generate a variety of nucleosome structures with functional consequences.

High mobility group proteins

High mobility group (HMG) proteins can be classified into three different families: HMGA, HMGB, and HMGN (A = AT-hook binding; B = box; N = nucleosome binding) [60]. They are a family of chromosomal architectural proteins that are extractable from chromatin with 0.35 M NaCl and 2–5% perchloric acid (PCA) and are often extracted together with histone H1 under these conditions. Their amino acid composition consists of approximately 50% hydrophilic amino acids, with the number of basic residues being slightly higher, and they exhibit higher interspecific variability than histones. HMGAs and HMGNs (Fig. 1E) provide good prototypes of IDPs as they exhibit very little, if any, secondary structure in solution [61, 62]. HMGBs consist of a short N-terminal IDR followed by two globular DNA-binding domains, linked by a second short IDR and a 40–50 IDR, highly enriched in E/D residues, at their C-terminal end [63]. The molecular mass of HMGs is lower than 30 kDa, and hence, they have high mobility in polyacrylamide gels. They contribute to mediate accessibility to DNA within chromatin and therefore play a role in the regulation of multiple nuclear processes such as replication, transcription, DNA recombination and repair [64, 65]. In this regard, HMGN1 and HMGN2 have been shown to participate in the establishment of chromatin DNase I hypersensitive sites (DHSs), which are landmarks of genes poised for and/or activated transcription, and are present in promoters and enhancers [66].

After histones, they are the most abundant of the non-histone proteins associated with chromatin [65], with an approximate average of 10^6 molecules per cell [47]. In rat tissues, HMGA and HMGB are each present at an approximate ratio of 0.2 molecules per nucleosome, and HMGN is present at approximately 0.5 molecules per nucleosome [67]. Although initially thought to be ubiquitously distributed throughout eukaryotes, HMGN canonical sequences have only been described in vertebrates, where they constitute a family of rapidly evolving nucleosome-binding proteins [68], while HMGA and HMGB have also been described in *Drosophila* [69] and in plants [70]. Nucleosome binding IDRs containing short HMGN sequences have recently been described in tardigrades, where they were preferentially found in enhancers and promoters [71]. Interestingly, the motif found in tardigrades corresponds to the RRSARLSA motif, which is present in MGN proteins. It is responsible for the recognition and binding to the acidic patch of the nucleosome, suggesting it to be an ancestral motif for chromatin binding [72].

So far, only HMGA1, in particular its HMGA1a isoform, has been shown to nucleate into foci within the nucleus and to undergo LLPS in vitro readily [73]. Although initially only AT-hooks 2 and 3 have been involved, the process likely involves all three of them within the protein IDR, as AT-hook 1 has been shown to play a critical role in the binding of HMGA to neighbouring DNA molecules [74].

Protamines

Protamines are relatively small (~ 3,000–10,000 Da) arginine-rich proteins [75] that are ubiquitously present in the sperm in the chromatin of many vertebrate and invertebrate organisms [76] [see [77] for a brief recent overview] and in some plants [78]. Quite often, they arise from post-translational cleavage of a larger protamine-like (PL) precursor (Fig. 1C) that is evolutionarily related to the replication-independent histone H5 (Fig. 1B) [79], which is present in the nuclei of the terminally differentiated erythrocytes that retain the nuclei in vertebrate species.

Protamines are highly disordered proteins (> 80% disorder) (Fig. 1D, H), and as it is characteristic of proteins consisting of IDRs, these regions can often adopt secondary structure upon interaction with their binding partners (i.e. DNA) [80].

Intrinsically disordered protein regions, and in particular their PTMs (i.e., phosphorylation), are involved in phase separation [81–84] and structural chromatin proteins are not an exception. For instance, histones and protamines have now been well documented to impart LLPS on chromatin, as will be discussed in the next section.

Chromatin readers

Histones, and in particular their IDRs, are subject to a plethora of PTMs [85, 86] that include, amongst others, acetylation, methylation, phosphorylation and ubiquitination. The unmodified core histone tail collapses onto the nucleosome, potentially increasing the alpha-helicity of the tail [87]. In the acetylated state, the core histone tail exhibits increased alpha-helicity [88] and extends from the nucleosomal DNA, making it available for binding by readers such as BRD4. In vitro studies provide evidence that the contribution of the core histone tail to phase separation is dependent on the charge and position of the PTM [89]. In addition to histone PTMs, DNA in the nucleosome is read by proteins that bind to methylated DNA, in particular methylated CpG, a DNA modification that regulates gene expression in a contextual sequence-dependent way [90]. Several readers carry enzymatic activity (e.g. KAT3, reader-writer; BRD4, reader-writer; KDM5A, reader-eraser; CHD1, reader-chromatin remodeler). We will highlight a few chromatin readers in which the IDR has a biological role.

BRD4, an acetyl lysine reader

BRD4, a bromodomain reader, plays a significant role in transcription, participating in multiple protein-protein interactions that mediate communication between enhancers and promoters [24]. BRD4 has two isoforms, the products of alternative splicing, distinguished by the presence or absence of a C-terminal tail extension. The BRD4 long isoform (BRD4-L) has a long C-terminal tail absent in the short isoform (BRD4-S). The BRD4 isoforms have different roles in cancer (e.g., BRD4-S has oncogenic activity, while BRD4-L has tumor growth suppressive activity in breast cancer) [91, 92] and in the regulation of viral gene expression [93]. On their N-termini, the BRD4 isoforms have two bromodomains followed by IDR domains. The bromodomains bind to acetylated lysines on the H4 tail [94]. The organization of the modules in the BRD4 N-terminus is: two bromodomains, followed by the N-terminal cluster of phosphorylation sites (NPS), a basic residue-enriched interaction domain (BID), an extra-terminal (ET) domain, and a C-terminal cluster of phosphorylation sites (CPS). The NPS and CPS IDR domains are rich in serine residues, whereas the BID IDR contains multiple lysines. These IDRs and the bromodomains are involved in LLPS formation. BRD4 forms puncta in nuclei. The BRD4-S and BRD4-L puncta colocalized with H3K27ac and MED1 (a subunit of the Mediator complex). Han et al. presented evidence that BRD4-S plays a greater role than BRD4-L in forming BRD4 condensates within chromatin [95]. The IDR of BRD-S was shown to contribute to BRD4's transcriptional function. Further, the authors show that the transcriptional requirement for BRD4-L or BRD4-S may be gene-specific [95].

Spindlin1, a methyl lysine reader

Spindlin1 (SPIN1) is a methyl-lysine reader (H3K4me3, H3K9me3) that plays a role in tumorigenesis. SPIN1 localizes to the nucleolus and in condensates in the nucleoplasm. SPIN1 has an N-terminal IDR, which is required to form SPIN1 condensates and enhances SPIN1 binding to H3K4me3. The SPIN1 IDR also contributed to the localization of SPIN1 to promoter regions [96] and the activation of tumorigenesis-related genes [56]. Histone methyltransferase MLL1 is recruited to the phase-separated SPIN1, with the activity of MLL1 increasing H3K4me3.

MeCP2

Methyl CpG binding protein 2 (MeCP2) is a chromosomal protein that, as its name indicates, binds preferentially to methylated CpG regions of the genome of

vertebrates [97]. Mutations in MeCP2 are the primary cause of RETT syndrome [98]. However, the protein can also bind to non-methylated CpG [99, 100] and to non-CG methylated DNA [101, 102] in addition to binding to methylated [103, 104] and unmethylated histones [105]. In most somatic cells, the protein represents a small chromatin component. Nevertheless, in cortical neurons, the protein is present in almost equal amounts as histones, and hence, in these brain cells, the protein constitutes a *bona fide* chromosomal protein in terms of its abundance. The protein consists of a methyl-binding domain (MBD), which is surrounded by two highly unstructured N- and C-terminal domains that amount to approximately 60% disorder [106] (Fig. 1F-H).

The involvement of MeCP2 in LLPS has been recently studied quite extensively [107, 108] (reviewed in [109]). Such an involvement is not surprising given the highly disordered nature of MeCP2 (Fig. 1F-H) and of its large number of PTMs [110–112]. In addition to its IDR-2 domain [113], the process involves MeCp2 self-interaction and is restricted by DNA methylation [114].

NuRD

The nucleosome remodelling and deacetylase (NuRD) multiprotein complex (about 2 MDa) serves as a corepressor and coactivator [115] and has seven core subunits, each with multiple paralogs [116]. NuRD plays a role in development, cancer and aging [116]. The NuRD subunits and paralogs include chromodomain helicase DNA-binding protein (CHD1/2/3), metastasis-associated protein (MTA1/2/3), GATA2A/B, methyl-CpG-binding domain-containing protein (MBD2/3), histone deacetylase (HDAC1/2), RB binding protein (RBBP4/5), and cyclin-dependent kinase 2-associated protein (CDK2AP1/2). MBD2 and MBD3 have distinct IDRs and can promote LLPS [117]. IDRs within the NuRD subunits are involved in protein interactions within the NuRD complex or with protein networks. The MBD2 IDR serves as a protein-interaction region that recruits the HDAC core to the NuRD complex [73]. The N- and C-termini of the CHD proteins contain multiple IDRs. Tabar et al. reported that the IDRs establish distinct protein interactions [118]. The proteins interacting with the N-termini of the CHD proteins varied. The CHD1 N-terminus interacted with the TAT-binding associated factors, while the CHD3 N-termini interacted with the casein kinase II complex subunits. Similarly, the C-termini of the CHDs interacted with different proteins.

Wei et al. demonstrated that the MBD2 condensate plays an essential role in the assembly of the NuRD complex, the formation of MBD2-NuRD condensates, the enhancement of NuRD enzymatic activity, and chromatin condensation of targeted genomic regions. The MBD2 condensates were often positioned next to H3K9me3 foci; H3K9me3 is a mark of heterochromatin. In cancer cells, MBD2-NuRD was bound to methylated CpG islands associated with tumour suppressor genes. The methyl-binding domain, IDR, and C-terminal coiled-coil domain contributed to the coacervation of MBD2. The MBD2 coacervation was reversibly regulated by redox status. Treatment of cancer cell lines with pro-oxidative drugs (elesclomol, nelfinavir) diminished MBD2 puncta. These pro-oxidative drugs have shown utility in treating cancers with elevated MBD2 protein expression. Disruption of the MBD2-NuRD condensate by pro-oxidative drugs increased the expression of tumour suppressor genes. Oxidation of Cys 359 resulted in dispersion of the MBD2 condensate. Redox regulation is one mechanism that modulates condensates by altering IDR conformation and protein interactions [119, 120].

Heterochromatin proteins

H3K9me3 and H4K20me3 are repressive marks associated with constitutive heterochromatin. KMT1B (SUV39H2) and KMT5B (SUV420H1) catalyze the formation of H3K9me3 and H4K20me3, respectively. The H3K9me3 reader, HP1β, recruits KMT5B [24].

Initially discovered in *Drosophila* [121, 122], HP1 now constitutes a family of proteins (mammalian HP1α, β, and γ) [123, 124]. The different isoforms, in particular their globular chromodomain (CHD) and chromoshadow (CSD) domains, are highly conserved through evolution from *Saccharomyces* to mammals [124]. Their molecular mass ranges from 20 to 46 kDa [125], and their folded N-terminal (CHD) and C-terminal (CSD) domains [126] are connected and flanked by three IDRs [49] (Fig. 1G). They interact with chromatin through the interaction of their CHD with histone H3 tri-methylated at lysine 9 [127–129]. They participate in gene silencing and heterochromatin formation, in particular pericentric heterochromatin (PCH), through preferential interactions with histone variant H2A.Z [130]. Indeed, although members of the HP1 family have similar structures, their multifunctionality [131] relies on their ability to interact with different protein complexes [123].

Guthmann et al. applied a bioinformatic approach to identify proteins involved in constitutive heterochromatin [132]. Tapping into mass spectrometry data sets that had information about proteins binding to H3K9me3, H3K9me3 nucleosomes (+/- methylated DNA) or present in a sonication-resistant fraction of chromatin, the investigators identified 148 proteins that were present in several mass spectrometry studies. Among the 148 proteins, a search for orthologs in *Danio rerio*, *Saccharomyces pombe*, *Drosophila melanogaster* and *Caenorhabditis elegans* identified HP1 isoforms as a common heterochromatin protein. The 148 proteins were further characterized for IDRs using the prediction algorithms IUPRED

and PONDR. Strikingly, these heterochromatin proteins were rich in IDRs, with a mean percentage of total protein length *occupied by IDRs of 44%, which was higher* than that of nuclear proteins. The investigators reported that proteins binding to DNA or chromatin had longer lengths of disordered segments than most nuclear proteins. An analysis of known heterochromatin proteins for features supportive of phase separation identified a prion-like domain in ATRX and CBX5. The authors point out that, in addition to heterochromatin proteins with IDRs, RNA interactions with these proteins may also play a role in establishing a phase-separated domain.

Chromatin liquid-liquid and solid-like phase separation

In this section, we are going to focus mainly on the involvement of LLPS/SLPS in the formation of chromatin condensates in somatic and spermiogenic cells, as they represent the two extremes of chromatin organization resulting from the nucleosome structure imparted by histones and the non-nucleosome structure resulting from the drastic replacement of histones by protamines during spermiogenesis. LLPS/SLPS refer to the formation of chromatin condensates in which the chromatin fiber (nucleosomal or nuceoprotamine) undergo a phase separation-mediated association that results in either highly fluidic (liquid-liquid) or highly constrained immobile (solid-like) condensates The main structural components of somatic chromatin and in the female gamete (oocyte) are DNA and histones [47]. By contrast, in the sperm, the situation is more complex. Indeed, the main sperm nuclear basic proteins (SNBPs) that associate with DNA to result in the male gamete chromatin consist mainly of three different protein types: histones (H type), as some organisms retain histones in their sperm, protamine-like proteins (PL type) and protamines (P type). Therefore, while the nucleosome organization is maintained in the H type, in the PL or P type, no nucleosome structure results from their association with DNA. The reader is referred to [76, 133] for comprehensive reviews on this topic.

The theory behind phase separation

Liquid-liquid phase separation refers to the process by which a homogeneous liquid mixture of several components (one phase regime) spontaneously separates into two different phases of varying concentrations [i.e. C_L and C_D in Fig. 2A-B [134]]. The process is affected by the physical conditions of the environment such as pH, ionic strength, temperature or other biomolecules in the media that affect the concentrations at which the phases separate [see [135] for a more detailed description]. Over the years, LLPS has been shown to play a very important role in the compartmentalization of functionally relevant membrane-less biological condensates within the cell [136]. More recently, interest has grown in the study of its role in the organization of somatic chromatin [137] where a distinction has been made between LLPS and SLPS [138].

Figure 2 summarizes the fundamental aspects of LLPS [134] adapted to chromatin and its surrounding nucleoplasm within the somatic (Fig. 2A-C) and spermiogenic (Fig. 2D-F) cell nuclei.

For somatic cell LLPS, Fig. 2A was adapted from Fig. 3 of [139]. In this representation, the diagram shows a plot of the inverse of the nucleosome binding energy (E_0) as a function of the nucleosome concentration using a multiscale coarse-grained chromatin model with 12-mer nucleosome arrays and 25 bp linker DNA. The nucleosome binding energy E_0 is defined as the nucleosome binding energy which scales all the inter-nucleosomal interactions. Beyond the critical point (E_0 = 1.7 for the nucleosome array), no phase separation takes place. The color gradient of the area within the bimodal line depicts the transition from the liquid-like (LLPS) at $E_0 \leq 3.0$ to the solid-like (SLPS) at $E_0 \geq 4.0$ of the chromatin condensates in the D phase [139]. It is important to add here that the nucleosome spacing as measured by the length of the linker DNA plays a very important fine-tunning role in all of this [140]. Experimental observations have recently justified the utility of using in vitro models with short DNA fragments [141].

With the spermiogenic chromatin (Fig. 2D-F), the diagram shown in Fig. 2D adopted and modified from Fig. 4 in [76] shows a plot of the inverse of the interaction parameter χ (chi) as a function of concentration, where χ expresses the strength of the energetic interaction between the nucleoplasm and nucleoprotamine compartments. Spinodal decomposition (SD) is a very dynamic LLPS process that is observed in liquid crystals [142, 143] and in polymers [144, 145]. Spinodal decomposition has been also observed in organisms, where, during spermiogenesis, a sequential post-translational cleavage of a protamine PL precursor occurs, resulting in the smaller protamines present in the mature sperm (Figs. 2F and 3A-(d)) [76]. Thus, it is likely that this process is an important component in triggering the SD separation (Fig. 3A). In many organisms, SD is often followed by a further nucleation transition also involving LLPS (Figs. 2D and 3A-(b) 2), before reaching the full chromatin compaction observed in mature sperm (Figs. 2E-F and 3A-(c) 2.

Spinodal decomposition of spermiogenic chromatin

We begin with this chromatin type because, to the best of our knowledge, it provided the first description of a potential connection between chromatin and LLPS. In 2005, a very unusual chromatin organization was

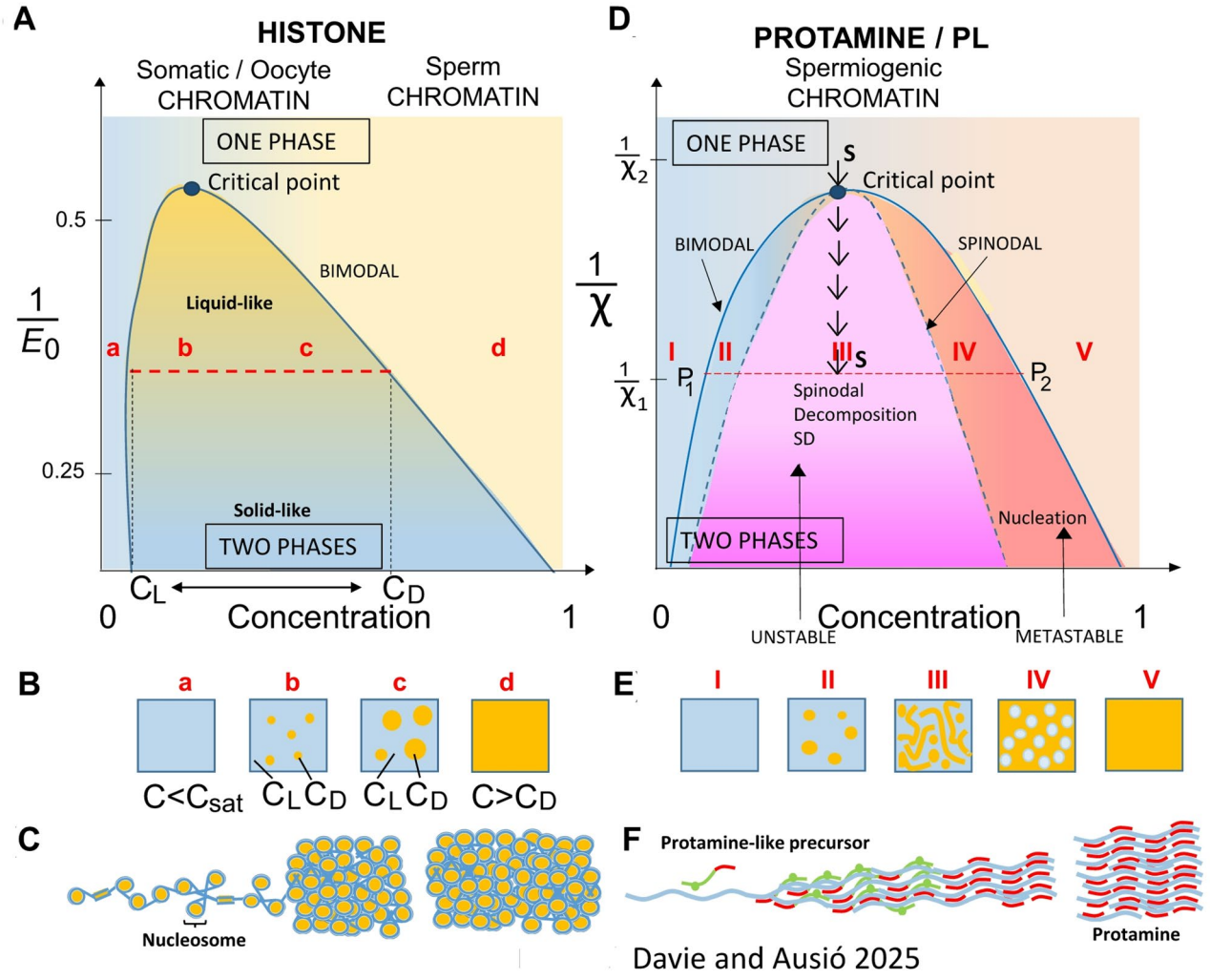

Fig. 2 Sketch of phase diagrams for somatic and sperm chromatin. **A** Schematic diagram for the liquid-liquid and the solid-like phase separation (LLPS/SLPS) of nucleosome organized chromatin. The bimodal line (blue) separates the one phase and two phases domains as a function of the nucleosome binding energy E_0 (see text for more details). No phase separation takes place beyond the critical point. Within the two phases regime, at a critical high E_0, a transition takes place from a liquid-liquid to a solid like phase separation of chromatin (see text). **B** At any different condition E_0 within the two-phases region on a single tie line (for instance on the red dotted line shown in (A)) the system disperses into light and dense phases of concentrations C_L and C_D with only their volume changing relatively to each other (a – d). (**C**) Molecular model of the chromatin condensation in the a to d transition shown in (**A**-**B**). Yellow color: Chromatin (nucleosomes); light blue background: interchromatin compartment. C_{sat} is the concentration above which the phase separation starts to take place. **D** Sketch for the LLPS of protamine/ protamine like (PL) spermiogenic chromatin. As in (**A**), the bimodal blue line separates the phase domains but as a function of the interaction parameter χ (chi). The spinodal (dashed blue line) encompasses the unstable region of instability where the system separates int two phases by spinodal decomposition (SD). A system at composition S above the phase separation curve at $1/\chi_1$ exists as one phase. However, if suddenly brought to $1/\chi_2$ (depicted by the sequential little arrows) it will split into two phases of compositions P1 and P2. In the area (in orange color) between the bimodal and spinodal line to the right, the system de-mixes by nucleation in a metastable state. **E** and **F** same as in (**B**-**C**). A protamine PL precursor is shown as a green-red molecule to be processed into a protamine (red) during spermiogenesis

observed in the transmission electron micrographs (TEM) cross-sections of the late spermatids of the gastropod snail *Murex brandaris* (spiny dye murex) (Fig. 3A-(a)) [146]. This unique chromatin organization was attributed to and demonstrated to be the result of spinodal decomposition [99], as described in the previous section. In sperm, this is a biochemically complex phenomenon that leads to the formation of a fluid-like highly dynamic lamellae (Fig. 3A-(a) 2–3, blue arrows). As for the fluidic aspects, a very recent publication has shown that double stranded dsDNA protamine condensates are liquid in the presence of single stranded ssDNA [147]. This has led to the hypothesis that the association of protamines with the numerous dsDNA breaks that are present in elongating spermatids, to remove the DNA supercoils [148] during the histone to protamine transition, form liquid condensates at this spermiogenesis stage [147]. Moreover, it has been shown that the

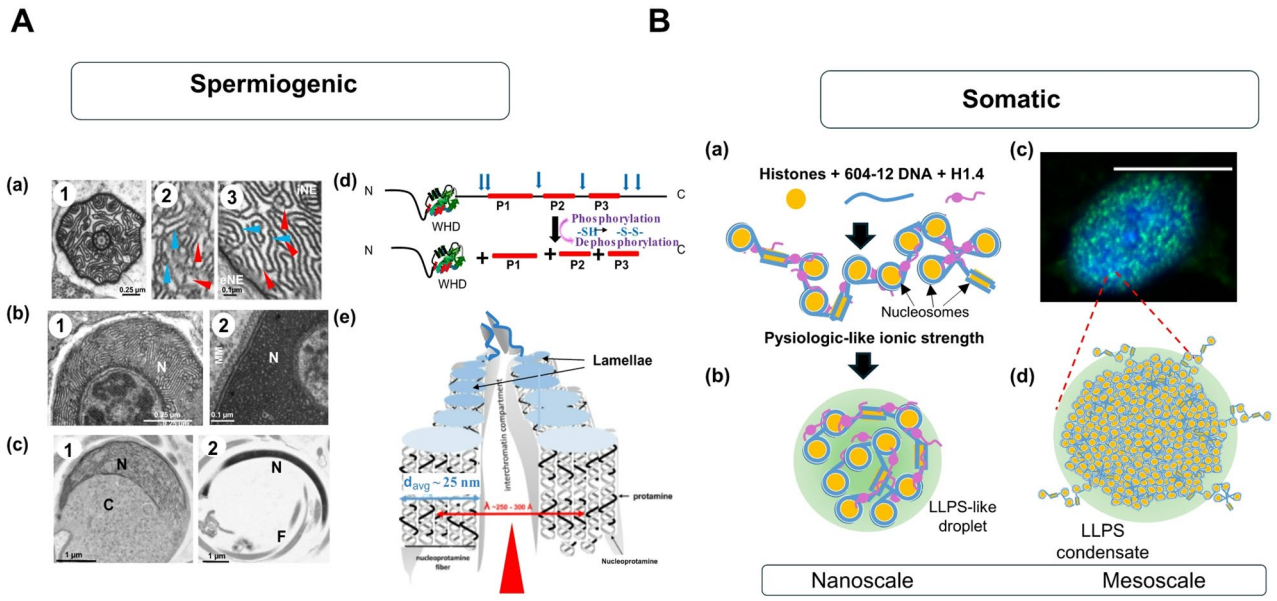

Davie and Ausió 2025

Fig. 3 Occurrence of chromatin LLPS in spermiogenic and somatic cells. **A** Widespread occurrence of chromatin spinodal decomposisition during spermiogenesis in several organisms. **a** Transmission electron microscopy (TEM) micrograph of a transverse section of the nucleus of an elongated spermatid of the gastropod *M. brandaris* [1] depicting the lamellar chromatin organization that is characteristic of spinodal decomposition (SD). Also shown are the dynamic disruption and reassembly involved in the process of remodelling of these structures corresponding to an internal region of the nucleus [2] and to the association of the lamellae with the nuclear envelope [3]. The blue and red arrowheads point to the lamella and to the interchromatin compartment respectively. eNE: external nuclear envelope; iNE internal nuclear envelope. **b** TEM of cross sections of late spermatids from the spider *Steatoda grossa* at different stages of chromatin condensation undergoing SD [1] and nucleation [2]. N, nucleus. **c** Electron micrographs of a condensing spermatid of *M. polymorpha* showing chromatin undergoing SD [1] and of a mature sperm cell [2] with highly condensed coiled nucleus (N) and flagellae (F). (**d**) Schematic representation of the protein processing from a PL precursor (pLP) into the final protamine P1-P3 during spermiogenesis. The (blue) arrows symbolize the cleavage sites. Other post-translational modifications such phosphorylation and cysteine oxidation are also indicated. WHD: winged helix domain. **e** Schematic cartoon representation of the dynamic lamellae seen in 3 A (**a**-**c**). The red arrowhead corresponds to the same arrowheads shown in (a) 2–3. (B) Phase separation of somatic chromatin in vitro and in vivo. **a** Chromatin reconstitution approach to reconstitute chromatin templates used in the in vitro analyses of LLPS/SLPS in solutions consisting of chemically defined environments. **b** Under these experimental conditions the reconstituted chromatin oligomers undergo SLPS/LLPS forming droplets as a result. (**c**) Immunofluorescence image of a nucleus from ReNCell neuronal cell line showing a characteristic punctuate pattern corresponding to chromatin condensates containing histone H1.4. DNA shown as a blue DAPI stain and the error bar is 10 µm. (**d**) Schematic representation of the corresponding chromatin condensate

packaging of DNA by protamines is a highly reversible process [149] that is likely impacted by the nucleoplasm through enzymes involved in protamine precursor cleavage and protamine PTMs (e.g. phosphorylation) hence affecting the two compartment interactions (Figs. 2F and 3A (d)). The interchromatin compartment (Fig. 3A-(a) 2–3, red arrows and Fig. 3A-(e)) [150] plays a crucial role, participating in both the formation of lamellar structures and shaping the functional organization of the spermiogenic nuclei. In *M. brandaris*, the process starts with the formation of fibro-granular structures of 15 nm of diameter [151] that coalesce into dynamic lamellae of approximately 25 nm thickness as those shown in Fig. 3A-(a) and schematically shown in Fig. 3A-(e). Interactions with the nuclear envelope play an important role (Fig. 3A-(a) 3) [151] in the appearance of the lamellar pattern. As shown in Fig. 3A-(b) and Fig. 3A-(c), spinodal decomposition has been observed in many other organisms, such as in the evolutionarily distant spider *Steatoda grossa* [77] and in the liverwort *Marchantia polymorpha* [78]. Figure 3A-(b) 1–2 correspond respectively to stages III and IV (nucleation) in Fig. 2E. In the liverwort (Fig. 3A-(c) the stages shown correspond to those of Fig. 2E, III and V (highly compacted chromatin in mature sperm). Beyond these three representative species, the process of spinodal decomposition is observed in the sperm of many other organisms from plants like algae [152] and the liverwort *Marchantia* [78] and in many invertebrate [77, 146, 153] and vertebrate organisms [76, 154] that exhibit an extensive post-translational processing of protamine

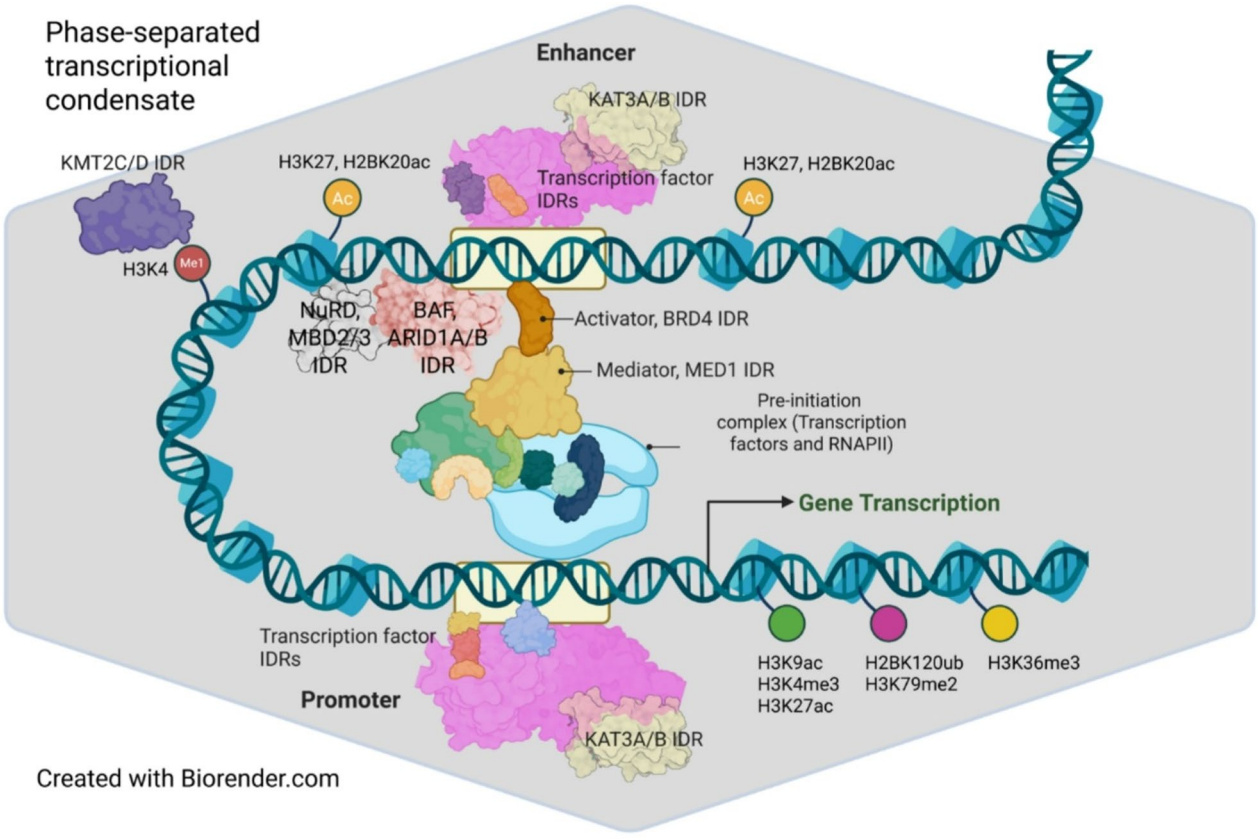

Fig. 4 Transcription condensates. Representation of enhancer–promoter interaction and the players involved in a transcriptional condensate. An active enhancer is associated with transcription factors, writers [KAT3A/3B (also known as CBP/p300); KMT2C/D (also known as MLL3/4)], erasers (NuRD), coactivators/readers (Mediator, KAT3A/3B, BRD4), active histone PTMs (H3K27ac, H4K20ac, H3K4me1), and chromatin remodelers (BAF and NuRD complexes). KAT3A/3B catalyzes the production of H3K27ac and H2BK20ac. KMT2C/D's product is H3K4me1. The upstream promoter region is associated with transcription factors and KAT3A/B. The pre-initiation complex is bound to the active promoter. Different writers are involved in the genesis of modified nucleosomes along the transcribed gene body, with the order of nucleosomal histone PTMs shown in the illustration. The IDRs of the proteins involved in a productive enhancer-promoter coupling contribute to the formation of a transcriptional condensate. Created by Biorender.com

precursors during their spermiogenesis (Fig. 3A-(d)) [76]. The mechanism often includes protein cleavage and PTMs such as phosphorylation (Fig. 3A-(d)).

Vertebrate sperm, like somatic cells can also exhibit the presence of chromatin condensates that take different shapes and conformations that can be visualized during the chromatin condensation process taking place during spermiogenesis and which are unrelated to SD. For instance in some fish containing protamines such as in the sea bass *Dicentrarchus labrax*, chromatin, condensates in the range of 150 ± 50 nm in diameter are present [155]. Other vertebrates, like birds and mammals exhibit rod-like and toroidal structures in which the rods have a width of 40–50 nm and the toroids are 40 nm thick and have an approximate diameter of 90 nm [156]. It is likely probable that these unique condensates are produced in a similar way by processes like those of somatic chromatin described in the next section. The uniqueness of their shapes being determined by the different protamine amino acid composition types present in each of these organisms [157].

Biomolecular condensate formation in somatic chromatin

The very long chromatin fibers behave like a viscoelastic polymer [158] and as such they are prone to aggregate [159]. However, in the case of somatic chromatin consisting of histones organized into nucleosome repetitive units, the dynamics of local functionally relevant domains can be simulated using chromatin fragment models such as those in Fig. 2A that might translate into chromatin dynamics in the cell [160]. In vitro evidence for the LLPS of chromatin using these model systems was initially described by the Rosen lab [161] using reconstituted complexes consisting of a defined DNA template and purified histones (Fig. 3B (a)-(b) similar to the chromatin models used in the elaboration of the data displayed in Fig. 2A [139]. Subsequently to this first publication another paper was published by a different lab which contradicted the earlier results and indicating that

chromatin condensates behave as a solid in the mesoscale and in living cells [162]. In all this experimental work, especial caution needs to be paid to the ionic conditions (i.e. ion composition and ionic strength) of the buffers as well as sample preparation details used [including DNA length [163]] that can affect the inter-nucleosomal interactions and ultimately determine their liquid-like or solid-like behavior as shown in Fig. 2A [139]. As it was pointed out in [160], the disagreement between the two publications could be accounted for by differences with the sample imaging and further support to the LLPS nature of the chromatin was provided [160]. Indeed, a very recent paper from the Rosen's lab has shed further light into the problem by elegantly showing that variation in the internucleosomal linker length affecting histone-tail interactions at the nanoscale (as it is the case of the in the in vivo setting at the mesoscale) (Fig. 3B) are behind chromatin condensate architecture and mechanics, a process affected by histone acetylation [164]. Interestingly, histone acetylation has the potential to weaken the nucleosome binding energy E_0 in Fig. 2A, in agreement with early structural observations made at the nucleosome scale [165, 166].

Chromatin behaves as a viscoelastic nucleoprotein polymer. The suitability of polymer chemistry to account for the formation of chromatin condensates, regardless of its histone or protamine protein composition has been long ago described [159]. Hence, despite the new theoretical approaches further developed more recently in this field to account for the chromatin compartmentalization by polymer-polymer phase separation (PPPS) [167], this is not a genuinely new concept. It is important to recognize, however, that it is such polymeric viscoelasticity that bestows chromatin with its dynamic and elastic properties of the nuclear condensates (Fig. 3B (d)) within the nuclear setting [158].

In vivo, in the nucleus, interaction of chromatin with specific partners, such as, for instance, specific histone H1 variants H1.4 and H1.5 (Fig. 3B (c)) [168, 169] or MecP2 [113], to provide just a couple of examples, can lead to LLPS-driven condensates. The histone H1.4 the foci exhibit a diameter of approximately 250 nm [168] (Fig. 3B (c)-(d)) which can be estimated to comprise approximately 7100 nucleosomes assuming each nucleosome to correspond to a sphere of 13 nm in diameter and taking into consideration a factor of 0.74 for the Kepler's correction for sphere packing (a schematic representation is shown in Fig. 3B (d) [170]. Interestingly, a few IDRs of MeCP2 have been shown to be involved in the MeCP2-driven condensates [113]. As suggested in [164], these condensates likely form through phase separation of small regions from one or more than one chromosomes and are consistent with TADs [171, 172].

A final consideration that affects both somatic and sperm cells has to do with the mechanical regulation of the dynamics of their chromatin condensates that can be affected by external cues such as osmotic pressure, nucleoplasm fluid flow and contractile forces from actomyosin. Conversely, within the same dynamic mechanisms, changes in the condensates can exert mechanical effects on chromatin and nuclear stiffness [173] a good example of which is provided by sperm chromatin [174, 175].

The need for further research on membraneless organelles and the role of IDPs/IDRs in their assembly still requires further research as recently pointed out by Uversky. The low resolution techniques used for the study of MLOs, which are stabilized by weak, transient multivalent, "touch-and-go" interactions between IDPs/IDRs and other biological macromolecules, it is like looking at a "fuzzy herd of fuzzy elephants" [176].

Somatic cell chromatin compartments

Chromatin is organized into compartments, with expressed genes localized in 'Euchromatin (compartment A)' and repressed genes in compartment B (heterochromatin). The nucleosome's structure and histone PTMs hold the information to form the two compartments [177] and enable their phase-separated chromatin immiscibility.

Euchromatin (compartment A)

Compartment A chromatin is associated with "active histone marks" (acetylated histones). For most expressed genes, there is an order in which the histone PTMs are associated with the gene body. Next to the transcription start site of expressed genes are nucleosomes with H3K4me3, H3K9ac, and H3K27ac (Fig. 4). Going further into the transcribed gene body are nucleosomes with H3K79me2 and H2BK120ub followed by nucleosomes with H3K36me3. A specific writer catalyzes each of these histone PTMs. Modification of the histone tail IDRs alters the structure and position of the tail, as well as its interaction with other proteins (e.g., readers). Acetylation and ubiquitination of histones are rapidly added and removed, contributing to the dynamics of condensate formation and dissolution [161].

Phase-separated transcriptional condensate

Most phase-separated transcriptional condensates (PST-condensate) (Fig. 4) form transiently with regulatory elements within compartment A. Several factors drive the formation of PST-condensates, including the IDRs of transcription factors, chromatin remodelers and modifiers, transcription coactivators, and transcription machinery [178]. The dynamic nature of the PST- condensate enables reconfiguration in response to both external and

internal environmental changes. In cancer, oncogenic fusion proteins forge the formation of "oncogenic" transcriptional condensate, which drives the expression of key genes (for example, *HOXA9* in acute myeloid leukemia). Changes in metabolism and cellular stresses will also impact transcription condensate formation [179]. In the formation and dissolution of the PST-condensate, several factors may be involved, including modification of the IDR and RNA [178]. Protein modification by poly(ADP-ribosyl)ation catalyzed by poly (ADP-ribose) polymerase and reversed by poly(ADP-ribose) glycohydrolase may be involved in PST-condensate formation and dissolution [24, 180]. Low levels of nascent RNA produced in the initial steps of transcription support PST-condensate formation, while transcriptional bursting and production of increased RNA levels would result in PST-condensate dissolution [178, 181]. Alternatively, non-coding RNA could be involved in the formation of PST-condensates [182]. Clearly, there is still much to be learned about the formation and dissolution of PST-condensates.

Gene transcription requires the formation of the pre-initiation complex (complex of TFIID/E/F/H). Several of the general transcription factors and subunits thereof have IDRs. The TFIIEα subunit of TFIIE has an acidic IDR required for its interaction with TFIIH.

Initial events in PST-condensate formation are the binding of transcription factors and chromatin remodelers to nucleosome-free regions of the targeted gene and its regulatory regions (enhancers, super-enhancers, promoters) [29]. Many of the histone-modifying enzymes have IDRs that are likely involved in the formation of the transcriptional condensate. KMT2D (also known as MLL4) catalyzed the mono-methylation of H3K4 at enhancers and super-enhancers. KMT2D has large patches of Q (cluster 11) [13]. The KMT2D supports enhancer activity independent of its catalytic activity to produce H3K4me1 [183]. It is conceivable that the IDR mediator complex of KMT2D is one of the critical functional domains of this enzyme in establishing active enhancers. Transcription factors at enhancers also recruit the mediator complex and KAT3A/3B (CBP/p300) [24, 184], which have cluster 11 Q-rich regions in their IDRs. Together, the IDRs of these proteins regulate biomolecular condensate formation and transcriptional activity of genes [185].

Enhancers and super-enhancers, along with the proteins associated with these regulatory regions, are involved in the formation of transient macromolecular condensates. Transcription factors, MED1 of mediator, and reader of acetylated lysines, BRD4, have IDRs which contribute to the formation of the condensate [186, 187]. The majority of eukaryotic transcription factors have one or more IDRs [187]. Transcription factor binding to regulatory sites is governed by multiple mechanisms, including accessibility to the binding site within chromatin, typically in nucleosome-free regions, transcription factor modifications, and protein interactions (e.g. AP1 family of transcription factors). BRD4 has KAT activity and acetylates H3 at K122. However, when JNK phosphorylates BRD4 Thr1186 and Thr1212, BRD4 is dislodged from its chromatin site, disrupts its KAT activity, and associates with RNA polymerase II, and promotes BRD4's kinase activity [188]. Both threonines are within BRD4's IDR.

Super-resolution microscopy of live mouse embryonic stem cells has investigated the formation and dissolution of clusters comprising mediator and/or RNA polymerase II. The mediator is present in transient (11-second) clusters approximately 100 nm in diameter. Larger clusters (condensates) (about 300 nm) had either RNA polymerase II or mediator. The movies provided with this article show a dynamic interaction between the mediator cluster and *Esrrb* super-enhancer and *Esrrb* promoter, consistent with the dynamic kissing model for super–enhancer–promoter interactions [189]. A subsequent article by these authors demonstrated that the proximity of the mediator or RNA polymerase II condensates to the *Sox2* transcription site correlated with transcription burst size and frequency. In the three-way kissing model, the *Sox2* super-enhancer was in proximity to the *Sox2* promoter, and transcriptional bursts occurred when the RNA polymerase II moved to encompass the super-enhancer and promoter [190].

Replication-dependent histones are expressed in S phase in synchrony with DNA replication in the formation of new nucleosomes. Transcription of replication-dependent histone genes occurs within a specialized biomolecular condensate called the histone locus body (HLB) [191]. Nuclear Protein, Ataxia-Telangiectasia Locus protein (NPAT) plays a critical role in HLB formation. NPAT, which binds to the promoter region of the histone genes, recruits the TRAPP/mediator complex and KAT5 (TIP60). NPAT has several large IDR regions: [192]. The NPAT's C-terminus region binds to FLICE-associated huge protein (FLASH), which is also required for HLB formation. The importin subunit alpha-4 (IMA4, also known as KPNA3) binds to the nuclear localization signal of NPAT and regulates its nuclear import. Further, IAM4 suppresses NAPT condensation, preventing NPAT condensation in the cytoplasm [192]. Phosphorylation of NPAT by Cyclin E/Cdk2 plays a critical role in the replication-dependent histone transcription. This event is important to the HLB's formation and growth. Interestingly, the HLB persists after replication-dependent histone gene transcription ends. There is evidence that Cyclin E/Cdk2 plays a role in determining the size, organization and function of the HLB [191].

The review authored by Rippe and Papantonis highlighted similarities between transcription factories and PST-condensates [178]. First reported by Jackson et al. in 1993 and subsequently by other groups, multiple genes, nascent transcripts, and RNA polymerase II were present in discrete foci called transcription factories [193, 194]. Studies on transcription factories and PST-condensates have shown that both are often adjacent to nuclear speckles. Transcription factories and PST-condensates share the same set of proteins (transcription factors, mediator, BRD3/4, KAT3A/B, HDAC1/2, CDK9, chromatin remodelers). The active form of RNA polymerase II is located on the protein core surface [178]. Of note, Jackson and colleagues showed that transcription factories were associated with a nuclear substructure known as the nuclear matrix or nuclear skeleton [195–198]. Reversible histone acetylation was shown to be catalyzed by KATs and HDACs bound to the nuclear matrix/skeleton [199]. The existence of this nuclear substructure has been debated; however, the nuclear skeleton/matrix may well be the remnants of protein-protein-RNA condensates once chromatin has been removed.

Transcription elongation machinery

After the initiation of transcription, the C-terminal tail (an IDR, cluster 28) of the largest subunit (RPB1) of RNA polymerase II undergoes phosphorylation at the S5 position of the heptad repeat $Y_1S_2P_3T_4S_5P_6S_7$. RNA polymerase II travels about 40–100 nucleotides before pausing. The elongation factors, the DRB sensitivity-inducing factor (DSIF) and negative elongation factor (NELF), stabilize the paused RNA polymerase II. The subunits of DSIF are SPT5 and SPT4, and the subunits of NELF are NELF-A, NELF-B, NELF-C/D, and NELF-E. Activation of the paused polymerase is mediated by the kinase CDK9 subunit of P-TEFb, which phosphorylates NELF, SPT5 and S2 of the RPB1 IDR. P-TEFb is a heterodimer composed of CDK9 and cyclin T1, with the active form being present in the super elongation complex [200] NELF phosphorylation results in the removal of this complex from the elongating complex.

SPT5 has two IDRs; one located in the N-terminal region and the other in the C-terminal region. Removal of either of these IDRs results in a reduction of the RNA synthesis [201]. CDK9 phosphorylation of SPT5 occurs on its C-terminal and the linker region between the KOWx-4 and KOW5 domains [202]. SPT5 phosphorylation of the C-terminal IDR enhances the relocation of SPT5 from pausing condensate to an elongation condensate [201, 203].

The Facilitates Chromatin Transcription complex, FACT, is involved in transcriptional elongation by facilitating the removal and addition of the H2A/H2B dimer from the nucleosome during the passage of RNA polymerase II. The two subunits of FACT are SSRP1 and SPT16. SPT16 has two IDRs; one in the center of the protein and the other acidic IDR at its C-terminal [50]. SSRP1 has a C-terminal IDR, which can be divided into an acidic part and a basic part. The SSRP1's IDR has the HMG box, which binds to the nucleosome. The IDRs of these FACT subunits are required for the displacement of H2A/H2B from the nucleosome [50]. The SSRP1 IDR has several CK2-mediated phosphorylation sites. In the fully phosphorylated state, this IDR will not bind to nucleosomes, while partial phosphorylation states alter the affinity of this region to the nucleosome [204].

Chromatin remodelers

BAF (SWI/SNF) is an ATP-dependent chromatin remodeler involved in re-structuring of the nucleosome and/or removal of the octamer from DNA, allowing for transcription factor and other chromatin-associated proteins to bind the remodelled region. The subunits of BAF include the SMARCA4 (BRG1) or SMARCA2 (BRM), SMARCB1 BAF47, SMARCC1 BAF155, SMARCC2 BAF170, BAF250a/b (ARID1A/B). The 29 genes coding for the BAF subunits are frequently mutated in cancer and in neurodevelopmental diseases, with the ARID1 genes (*ARID1A* and *ARID1B*) being the highest [13].

ARID1A/B has two IDRs in its N-terminal region, with most mutations associated with cancer or neurodevelopmental diseases occurring in these IDRs. The loss of IDR1 resulted in changes in the targeting of the BAF complex and a reduction in the formation of nucleosome-free regions [13]. In AN3CA (dedifferentiated endometrial carcinoma) cells, nucleosome-free regions enriched in motifs for the AP-1, NF1 and TEAD transcription factors were most impacted. Patil et al.'s study demonstrated that the N-terminal IDR and DNA-binding domain of ARID1A/B contributed to the association of cBAF with distal enhancers and the chromatin structural changes in these regulatory regions [13]. Further, the N-terminal IDR played a role in condensate formation and the association of mediator, RNA polymerase II, KAT3B, and multiple transcription factors (TEAD1, NF1A, cJUN). These studies further demonstrated that the grammar (clusters 10, 11, and 28) of the ARID1A/B N-terminal IDR was crucial in recruiting transcription factors and KAT3B, as well as the proper targeting of the cBAF complex. However, the cBAF complex with the ARID1A/C IDR swapped with IDRs of other proteins did form condensates. The study demonstrates that the function of the IDR in condensate formation and protein interactions is distinct.

Heterochromatin (compartment B)

In addition to the nucleosome properties, histone H1 and the heterochromatin protein one (HP1) contribute to the structure of heterochromatin [205, 206].

HP1α has three IDRs, which are located at the protein's N-terminal tail, between the N-terminal chromodomain and the C-terminal chromo shadow domain (also called the hinge region), and at the C-terminal tail [49, 207]. The C-terminal chromo shadow domain of HP1α is involved in dimerization.

The HP1α dimer can bridge two neighbouring H3K9me3-containing nucleosomes, promoting chromatin condensation. It has been shown that HP1α dimers can undergo LLPS to condense chromatin into a transcriptionally repressed heterochromatin [208, 209]; a process that is mediated by the phosphorylation of the N-terminal IDR with the participation of the other two IDR domains [210]. The binding of the HP1α dimer to H3K9me3 is enhanced with the casein kinase 2-mediated phosphorylation of four serines located in HP1α's N-terminal tail IDR. The interaction of the phosphorylated serines with the positively charged lysines in the N-terminal chromodomain is essential for the HP1α to undergo LLPS.

Although several recent papers present evidence for phosphorylated HP1α being involved in phase-separated heterochromatin as well as in DNA-damage response in repairing DNA breaks in heterochromatin [207, 211, 212], it was reported that mouse heterochromatin compaction was independent of HP1α [213–215]. In reconciling the conflicting reports about the role of HP1α in LLPS and heterochromatin formation, Bensaha et al. demonstrated that while fission yeast Swi6 and *Drosophila* HP1a can drive heterochromatin coalescence by LLPS in mammalian cells, mouse HP1α did not [216]. Human and mouse HP1α have reduced intrinsic disorder compared to fission yeast Swi6 and HP1a, thereby reducing mammalian HP1α's ability to undergo LLPS. Furthermore, mammalian cells have increased levels of HP1 paralogs that counteract LLPS formation [206, 216]. The nature of the physicochemical interactions that govern the phase-separation behaviour of its different paralogs (HP1α, HP1β, and HP1γ) has only recently begun to be elucidated [217].

H1 undergoes liquid-liquid phase separation in the presence of DNA or nucleosomes [205]. H1 binds to HP1α, and this interaction is regulated by H1 PTMs. H1 phosphorylation hinders the interaction between these two proteins.

Nuclear bodies and chromatin organization

Nuclear bodies play a role in chromatin organization and structure (218). Within the human nucleolus are the short arms of the acrocentric chromosomes 13, 14, 15, 21, and 22, which code for the rDNA genes. Nucleolus-associated domains (NADs) are repressed chromatin regions associated with the histone post-translational modifications (PTMs) histone dimethylated at lysine 9 (H3K9me2) [24]. The nucleolus has three internal subcompartments (the fibrillar center (FC), the dense fibrillar component (DFC), and the granular component (GC)). The IDRs of the nucleolar proteins have different IDR sequences (grammars/codes) e.g., IDRs with D/E tracts or K-blocks with E-rich regions. Upstream binding transcription factor IDR has a D/E tract (located in FC); Ly1-antibody reactive IDR has a K/E block; nucleolin IDR has a D/E-tract and RG-rich (located in DFC); and nucleophosmin 1 IDR has a D/E tract (located in GC). The D/E track IDR can bind protons and lower the pH of the nucleolar compartments to 6.5, compared to a pH of 7.2 in the nucleoplasm. King et al. [28] propose that the proton gradient may influence the specificity of enzyme-catalyzed reactions. Of note, the H imidazole side chain has pK_a of 6.3. At pH 6.5, the imidazole side chain is slightly positively charged, while at pH 7.2, the side chain is mostly neutral. The charge of the H side chain influences protein structure and protein interactions [218].

Fibrillarin, nucleolin, GAR1, and nucleophosmin are key nucleolar proteins with IDRs involved in phase separation [219, 220]. Fibrillarin is present in the DFC. The IDR within fibrillarin's (glycine and arginine rich) GAR domain promotes phase separation. The IDR is involved in fibrillarin self-association and in interactions with proteins and RNAs [221]. Nucleolin is present in the GC. Nucleolin has two IDR; the N-terminal IDR has four acidic tracts [222] while the C-terminal IDR is rich in arginine and glycine repeats. GAR1, like fibrillarin and nucleolin, is an RG/RGG nucleolar protein. The C-terminal RG/RGG repeats are required for phase separation and sub-nucleolar compartmentalization [223]. Nucleolin, fibrillarin and GAR1 have a phenylalanine-rich motif present in the RG/RGG motif.

90% of the most highly expressed genes are, to some extent, associated with nuclear speckles, a biomolecular condensate [224–226]. Nuclear speckles (also called interchromatin granule clusters) house splicing and transcription factors [227], and range from 25 to 50 per cell [224]. SRRM2 and SON play essential roles in nuclear speckle formation. The SSRM2 and SON protein structures are primarily disordered. The IDRs of SSRM2 and SON have R patches (cluster 26) [35]. The two proteins differ in that SSRM2 is largely positively charged, while SON is negatively charged. SSRM2 has serine/arginine-rich (RS)1 and RS2 domains on either side of the IDR [228]. Oligomerization by the RS domains is required for SSRM2 phase separation and nuclear speckle condensation. Functional nuclear speckles are formed when SRRM2 condensates coexist with SON as dense phases.

Concluding remarks

As early as in 1982, Grau et al.. made an observation according to which, in the presence of 0.5 mM $MgCl_2$ dinucleosomes gave rise to complexes of about 40 nm in diameter resembling those found in native chromatin [229]. Although there was no obvious explanation for it at the time, in 2016, linear 12-mer nucleosomal arrays in the presence of magnesium were similarly shown to assemble into reversible globular complexes that range in size from ~ 50 nm to ~ 2000 nm [230]. Interestingly, in the elaboration of the model described here to account for the somatic chromatin LLPS and SLPS, in Fig. 2A [139] the authors used 12-mer nucleosome arrays and the change in the nucleosome binding energy of all the internucleosomal interactions (which requires the minimum presence of a dinucleosome) as a function of the concentration for their analysis. The interesting coincidence of all of this, confers legitimacy to this model while providing an important theoretical framework towards our further understanding of the association behavior of the chromatin fiber and the nuclear condensates it forms. In this process, the intrinsic disorder of the histones [231], like with sperm protamines [76], play a critically important role and provide a very good example of the connection between LLPS and protein IDRs as discussed in this review.

Abbreviations

AF4	ALF Transcription Elongation Factor 4
AP-1	Activator protein 1
ARID1A/B	AT-rich interactive domain-containing protein 1 A/B; BAF, BRG1- or BRM-associated factors
BCOR	BCL6 corepressor
BRD4	Bromodomain-containing protein 4
CBX8	Chromobox protein homolog 8
CBP	CREB binding protein
CDK2AP1/2	Cyclin-dependent kinase 2-associated protein (1/2)
CHD	Chromodomain
CHD1	Chromodomain helicase DNA-binding protein 1
cJun	Oncogene c-jun
CSD	Chromoshadow domain
DFC	Dense fibrillar component
DHS	DNase I hypersensitive sites
dsDNA	Double stranded DNA
DSIF	DRB (double stranded RNA binding) sensitivity-inducing factor
Esrrb	Estrogen-related receptor beta
FACT	Facilitates chromatin transcription
FC	Fibrillar center
FUS	RNA-binding protein fused in sarcoma
GATA	GATA binding transcription factor family
GC	granular component
HDAC	Histone deacetylase
HF	Histone fold
HLB	Histone locus body
HMG	High mobility group
HOXA9	Homeobox protein 9
HP1	Heterochromatin protein 1
IDP	Intrinsically disordered protein
IDR	Intrinsically disordered region
KAT	Lysine acetyl transferase
KMT	Lysine methyl transferase
KOW	Kyrpides-Ouzounis-Woese
LLPS	Liquid liquid phase separation
MBD	Methyl binding domain
MBD2/3	Methyl-CpG-binding domain-containing proteins (2/3)
MeCP2	Methyl CpG binding protein 2
MED1	Mediator of RNA polymerase II transcription subunit 1
MLLT3	Myeloid/lymphoid or mixed-lineage leukemia translocated to chromosome 3 protein
MLOs	Membrane less organelles
MTA	Metastasis-associated protein
NAD	Nucleolus associated domain
NARDINI	Non-random arrangement of residues in disordered regions inferred using numerical intermixing
NELF	Negative elongation factor
NF1	Neurofibromin 1
NuRD	Nucleosome remodeling and de-acetylase
P	Protamine
PCH	Pericentric heterochromatin
PL	Protamine like protein
PLD	Prion-like domains
PPPS	Polymer-polymer phase separation
P-TEFb	Positive transcription elongation factor b
PTM	Post-translational modification
RB	Retinoblastoma
RBP	RB binding protein
RFdiffusion	RoseTTAFold diffusion
SD	Spinodal decomposition
RPB1	RNA polymerase II subunit B1
SLPS	Solid-like phase separation
SMARC	SWI/SNF-related matrix-associated actin-dependent regulator of chromatin
SNBP	Sperm nuclear basic protein
Sox2	SRY (sex determining region Y)-box 2
SPIN1	Spindlin-1; SPT5, suppressor of Ty5 homolog; SPT16, Suppressor Of Ty 16 Homolog
ssDNA	Single stranded DNA
TADs	Topologically associating domains
TEAD	TEA (TEF-1 and AbaA) domain transcription factor
TEM	Transmission electron micrographs
SSRP1	Structure specific recognition protein 1
TF	Transcription factor
WHD	Winged helix domain
YEATS	Yaf9, ENL, AF9, Taf14, Sas5 domain

Acknowledgements

The funder had no role in the design of the study, interpretation of the data, and the writing of the manuscript. We apologize to our colleagues whom we could not cite due to space constraints.

Author contributions

JA and JRD have both equally contributed to the writing and conceptualization of this paper.

Funding

This work was funded by Natural Science and Engineering Research Council of Canada (NSERC), Grant RGPIN-2017-04162 to JA and a NSERC Discovery Grant RGPIN-2023-04780 to JRD.

Data availability

No new data were generated or analyzed in this review.

Declarations

Consent for publication

All the authors have approved the manuscript prior to publication.

Competing interests

The authors declare no competing interests.

Received: 22 September 2025 / Accepted: 11 March 2026
Published online: 28 March 2026

References

1. Holehouse AS, Kragelund BB. The molecular basis for cellular function of intrinsically disordered protein regions. Nat Rev Mol Cell Biol. 2024;25(3):187–211.
2. Vazquez DS, Toledo PL, Gianotti AR, Ermacora MR. Protein conformation and biomolecular condensates. Curr Res Struct Biol. 2022;4:285–307.
3. Feng Z, Chen X, Wu X, Zhang M. Formation of biological condensates via phase separation: Characteristics, analytical methods, and physiological implications. J Biol Chem. 2019;294(40):14823–35.
4. Wang B, Zhang L, Dai T, Qin Z, Lu H, Zhang L, et al. Liquid-liquid phase separation in human health and diseases. Signal Transduct Target Ther. 2021;6(1):290.
5. Wright PE, Dyson HJ. Intrinsically unstructured proteins: re-assessing the protein structure-function paradigm. J Mol Biol. 1999;293(2):321–31.
6. Dunker AK, Lawson JD, Brown CJ, Williams RM, Romero P, Oh JS, et al. Intrinsically disordered protein. J Mol Graph Model. 2001;19(1):26–59.
7. Uversky VN, Gillespie JR, Fink AL. Why are natively unfolded proteins unstructured under physiologic conditions? Proteins. 2000;41(3):415–27.
8. Tompa P. Intrinsically unstructured proteins. Trends Biochem Sci. 2002;27(10):527–33.
9. Chouard T. Structural biology: Breaking the protein rules. Nature. 2011;471(7337):151–3.
10. Madhurima K, Nandi B, Munshi S, Naganathan AN, Sekhar A. Functional regulation of an intrinsically disordered protein via a conformationally excited state. Sci Adv. 2023;9(26):eadh4591.
11. Theillet FX, Kalmar L, Tompa P, Han KH, Selenko P, Dunker AK, et al. The alphabet of intrinsic disorder: I. Act like a Pro: On the abundance and roles of proline residues in intrinsically disordered proteins. Intrinsically Disord Proteins. 2013;1(1):e24360.
12. van der Lee R, Buljan M, Lang B, Weatheritt RJ, Daughdrill GW, Dunker AK, et al. Classification of intrinsically disordered regions and proteins. Chem Rev. 2014;114(13):6589–631.
13. Patil A, Strom AR, Paulo JA, Collings CK, Ruff KM, Shinn MK, et al. A disordered region controls cBAF activity via condensation and partner recruitment. Cell. 2023;186(22):4936–e5526.
14. Zhai Z, Meng F, Kuang J, Pei D. Phase Separation in Chromatin Organization and Human Diseases. Int J Mol Sci. 2025;26(11).
15. Sabari BR, Hyman AA, Hnisz D. Functional specificity in biomolecular condensates revealed by genetic complementation. Nat Rev. 2025;26(4):279–90.
16. Mensah MA, Niskanen H, Magalhaes AP, Basu S, Kircher M, Sczakiel HL, et al. Aberrant phase separation and nucleolar dysfunction in rare genetic diseases. Nature. 2023;614(7948):564–71.
17. Alberti S, Hyman AA. Biomolecular condensates at the nexus of cellular stress, protein aggregation disease and ageing. Nat Rev Mol Cell Biol. 2021;22(3):196–213.
18. Kilgore HR, Chinn I, Mikhael PG, Mitnikov I, Van Dongen C, Zylberberg G, et al. Protein codes promote selective subcellular compartmentalization. Volume 387. New York, NY: Science; 2025. pp. 1095–101. 6738.
19. De La Cruz N, Pradhan P, Veettil RT, Conti BA, Oppikofer M, Sabari BR. Disorder-mediated interactions target proteins to specific condensates. Mol Cell. 2024;84(18):3497–512. e9.
20. Vernon RM, Chong PA, Tsang B, Kim TH, Bah A, Farber P et al. Pi-Pi contacts are an overlooked protein feature relevant to phase separation. eLife. 2018;7.
21. De Sancho D, Lopez X. Crossover in aromatic amino acid interaction strength between tyrosine and phenylalanine in biomolecular condensates. eLife. 2025;14.
22. Shan L, Li P, Yu H, Chen LL. Emerging roles of nuclear bodies in genome spatial organization. Trends Cell Biol. 2024;34(7):595–605.
23. Chakraborty S, Mishra J, Roy A, Niharika, Manna S, Baral T, et al. Liquid-liquid phase separation in subcellular assemblages and signaling pathways: Chromatin modifications induced gene regulation for cellular physiology and functions including carcinogenesis. Biochimie. 2024;223:74–97.
24. Davie JR, Sattarifard H, Sudhakar SRN, Roberts CT, Beacon TH, Muker I, et al. Basic Epigenetic Mech Subcell Biochem. 2025;108:1–49.
25. Zhang Y, Stoppelkamp I, Fernandez-Pernas P, Allram M, Charman M, Magalhaes AP et al. Probing condensate microenvironments with a micropeptide killswitch. Nature. 2025.
26. Ye S, So CL, Cai D. Cracking the protein compartmentalization code with ProtGPS. Trends Biochem Sci. 2025;50(5):369–71.
27. Kappel K, Strebinger D, Edmonds KK, Chau-Duy-Tam Vo S, Vockley CM, Biswas T, et al. Characterizing protein sequence determinants of nuclear condensates by high-throughput pooled imaging with CondenSeq. Nat Methods. 2025;22(7):1464–75.
28. King MR, Ruff KM, Lin AZ, Pant A, Farag M, Lalmansingh JM, et al. Macromolecular condensation organizes nucleolar sub-phases to set up a pH gradient. Cell. 2024;187(8):1889–906. e24.
29. Li J, Liu S, Kim S, Goell J, Drum ZA, Flores JP et al. Biomolecular condensation of human IDRs initiates endogenous transcription via intrachromosomal looping or high-density promoter localization. Nucleic Acids Res. 2025;53(4).
30. Shi M, Wu Z, Zhang Y, Li T. Decoding intrinsically disordered regions in biomolecular condensates. Fundamental Research. 2025;in press.
31. Martin EW, Holehouse AS, Peran I, Farag M, Incicco JJ, Bremer A, et al. Valence and patterning of aromatic residues determine the phase behavior of prion-like domains. Volume 367. New York, NY: Science; 2020. pp. 694–9. 6478.
32. Naderi J, Magalhaes AP, Kibar G, Stik G, Zhang Y, Mackowiak SD, et al. An activity-specificity trade-off encoded in human transcription factors. Nat Cell Biol. 2024;26(8):1309–21.
33. Cohan MC, Shinn MK, Lalmansingh JM, Pappu RV. Uncovering Non-random Binary Patterns Within Sequences of Intrinsically Disordered Proteins. J Mol Biol. 2022;434(2):167373.
34. Zarin T, Strome B, Peng G, Pritisanac I, Forman-Kay JD, Moses AM. Identifying molecular features that are associated with biological function of intrinsically disordered protein regions. eLife. 2021;10.
35. Ruff KM, King MR, Ying AW, Liu V, Pant A, Lieberman WE et al. Molecular grammars of predicted intrinsically disordered regions that span the human proteome. Cell. 2025.
36. Owen I, Shewmaker F. The Role of Post-Translational Modifications in the Phase Transitions of Intrinsically Disordered Proteins. Int J Mol Sci. 2019;20(21).
37. Zhang M, Gu Z, Sun Y, Dong Y, Chen J, Shu L, et al. Phosphorylation-dependent charge blocks regulate the relaxation of nuclear speckle networks. Mol Cell. 2025;85(9):1760–74. e7.
38. Mar M, Nitsenko K, Heidarsson PO. Multifunctional Intrinsically Disordered Regions in Transcription Factors. Chemistry. 2023;29(21):e202203369.
39. Ortega E, Rengachari S, Ibrahim Z, Hoghoughi N, Gaucher J, Holehouse AS, et al. Transcription factor dimerization activates the p300 acetyltransferase. Nature. 2018;562(7728):538–44.
40. Lin R, Barrows D, Mo Y, Onikubo T, Zhang Z, Roeder RG. MED1 IDR acetylation reorganizes the transcription preinitiation complex, rewires 3D chromatin interactions and reprograms gene expression. bioRxiv. 2024.
41. Garcia Ramirez M, Rocchini C, Ausió J. Modulation of chromatin folding by histone acetylation. J Biol Chem. 1995;270(30):17923–8.
42. Chhetri KB, Jang YH, Lansac Y, Maiti PK. Effect of phosphorylation of protamine-like cationic peptide on the binding affinity to DNA. Biophys J. 2022;121(24):4830–9.
43. Ahmed SS, Rifat ZT, Lohia R, Campbell AJ, Dunker AK, Rahman MS, et al. Characterization of intrinsically disordered regions in proteins informed by human genetic diversity. PLoS Comput Biol. 2022;18(3):e1009911.
44. Orand T, Jensen MR. Binding mechanisms of intrinsically disordered proteins: Insights from experimental studies and structural predictions. Curr Opin Struct Biol. 2025;90:102958.
45. Skupien-Rabian B, Jankowska U, Swiderska B, Lukasiewicz S, Ryszawy D, Dziedzicka-Wasylewska M, et al. Proteomic and bioinformatic analysis of a nuclear intrinsically disordered proteome. J Proteom. 2016;130:76–84.
46. Torrente MP, Zee BM, Young NL, Baliban RC, LeRoy G, Floudas CA, et al. Proteomic interrogation of human chromatin. PLoS ONE. 2011;6(9):e24747.
47. van Holde KE. Chromatin. NY: Springer-; 1988.
48. Arents G, Moudrianakis EN. The histone fold: a ubiquitous architectural motif utilized in DNA compaction and protein dimerization. Proc Natl Acad Sci USA. 1995;92(24):11170–4.
49. Musselman CA, Kutateladze TG. Characterization of functional disordered regions within chromatin-associated proteins. iScience. 2021;24(2):102070.
50. Okuda M, Tsunaka Y, Nishimura Y. Dynamic structures of intrinsically disordered proteins related to the general transcription factor TFIIH, nucleosomes, and histone chaperones. Biophys Rev. 2022;14(6):1449–72.
51. Kasinsky HE, Lewis JD, Dacks JB, Ausió J. Origin of H1 linker histones. Faseb Journal: Official Publication Federation Am Soc Experimental Biology. 2001;15(1):34–42.
52. Ramakrishnan V, Finch JT, Graziano V, Lee PL, Sweet RM. Crystal structure of globular domain of histone H5 and its implications for nucleosome binding. Nature. 1993;362(6417):219–23.

53. Jumper J, Evans R, Pritzel A, Green T, Figurnov M, Ronneberger O, et al. Highly accurate protein structure prediction with AlphaFold. Nature. 2021;596(7873):583–9.
54. Fleming J, Magana P, Nair S, Tsenkov M, Bertoni D, Pidruchna I, et al. AlphaFold Protein Structure Database and 3D-Beacons: New Data and Capabilities. J Mol Biol. 2025;437(15):168967.
55. Chavez-Garcia C, Henin J, Karttunen M. Multiscale Computational Study of the Conformation of the Full-Length Intrinsically Disordered Protein MeCP2. J Chem Inf Model. 2022;62(4):958–70.
56. Gao J, Li H, Tan S, Zhou R, Lee TH. Roles of histone chaperone Nap1 and histone acetylation in regulating phase-separation of nucleosome arrays. Nat Commun. 2025;16(1):10672.
57. Gibbs EB, Kriwacki RW. Linker histones as liquid-like glue for chromatin. Proc Natl Acad Sci USA. 2018;115(47):11868–70.
58. Watson M, Stott K. Disordered domains in chromatin-binding proteins. Essays Biochem. 2019;63(1):147–56.
59. Strahl BD, Allis CD. The language of covalent histone modifications. Nature. 2000;403(6765):41–5.
60. Bustin M. Revised nomenclature for high mobility group (HMG) chromosomal proteins. Trends Biochem Sci. 2001;26(3):152–3.
61. Reeves R. Molecular biology of HMGA proteins: hubs of nuclear function. Gene. 2001;277(1–2):63–81.
62. Rochman M, Taher L, Kurahashi T, Cherukuri S, Uversky VN, Landsman D, et al. Effects of HMGN variants on the cellular transcription profile. Nucleic Acids Res. 2011;39(10):4076–87.
63. Starkova TY, Polyanichko AM, Artamonova TO, Tsimokha AS, Tomilin AN, Chikhirzhina EV. Structural Characteristics of High-Mobility Group Proteins HMGB1 and HMGB2 and Their Interaction with DNA. Int J Mol Sci. 2023;24(4).
64. Reeves R. Nuclear functions of the HMG proteins. Biochim Biophys Acta. 2010;1799(1–2):3–14.
65. Ozturk N, Singh I, Mehta A, Braun T, Barreto G. HMGA proteins as modulators of chromatin structure during transcriptional activation. Front Cell Dev Biol. 2014;2:5.
66. Martinez de Paz A, Ausio J. HMGNs: The enhancer charmers. BioEssays. 2016;38(3):226–31.
67. Kuehl L, Salmond B, Tran L. Concentrations of high-mobility-group proteins in the nucleus and cytoplasm of several rat tissues. J Cell Biol. 1984;99(2):648–54.
68. Gonzalez-Romero R, Eirin-Lopez JM, Ausio J. Evolution of high mobility group nucleosome-binding proteins and its implications for vertebrate chromatin specialization. Mol Biol Evol. 2015;32(1):121–31.
69. Ner SS, Churchill ME, Searles MA, Travers AA. dHMG-Z, a second HMG-1-related protein in Drosophila melanogaster. Nucleic Acids Res. 1993;21(18):4369–71.
70. Antosch M, Mortensen SA, Grasser KD. Plant proteins containing high mobility group box DNA-binding domains modulate different nuclear processes. Plant Physiol. 2012;159(3):875–83.
71. Cantara S, Regoli T, Ricci C. Captain Tardigrade and Its Shield to Protect DNA. DNA. 2025;5(2):27.
72. Alegrio-Louro J, Cruz-Becerra G, Kassavetis GA, Kadonaga JT, Leschziner AE. Structural basis of nucleosome recognition by the conserved Dsup and HMGN nucleosome-binding motif. Genes & development; 2025.
73. Zhu H, Narita M, Joseph JA, Krainer G, Arter WE, Olan I, et al. The Chromatin Regulator HMGA1a Undergoes Phase Separation in the Nucleus. ChemBioChem. 2023;24(1):e202200450.
74. Nue-Martinez JJ, Maturana M, Lagartera L, Rodriguez-Gutierrez JA, Boer R, Campos JL, et al. Crystal structure of the HMGA AT-hook 1 domain bound to the minor groove of AT-rich DNA and inhibition by antikinetoplastid drugs. Sci Rep. 2024;14(1):26173.
75. Balhorn R. The protamine family of sperm nuclear proteins. Genome Biol. 2007;8(9):227.
76. Kasinsky HE, Eirin-Lopez JM, Ausio J. Protamines: structural complexity, evolution and chromatin patterning. Protein Pept Lett. 2012;18(8):755–71.
77. Leyden MR, Michalik P, Baruffaldi L, Mahmood S, Kalani L, Hunt DF et al. The protamines of the spider Steatoda sp. provide an example of liquid-liquid phase separation chromatin transitions during spermiogenesis. Development. 2024;151(22).
78. D'Ippolito RA, Minamino N, Rivera-Casas C, Cheema MS, Bai DL, Kasinsky HE, et al. Protamines from liverwort are produced by post-translational cleavage and C-terminal di-aminopropanelation of several male germ-specific H1 histones. J Biol Chem. 2019;294(44):16364–73.
79. Eirín-López JM, Frehlick LJ, Ausió J. Protamines, in the footsteps of linker histone evolution. J Biol Chem. 2006;281:1–4.
80. Roque A, Ponte I, Suau P. Secondary structure of protamine in sperm nuclei: an infrared spectroscopy study. BMC Struct Biol. 2012;11:14.
81. Martin EW, Holehouse AS. Intrinsically disordered protein regions and phase separation: sequence determinants of assembly or lack thereof. Emerg Top Life Sci. 2020;4(3):307–29.
82. Ibrahim AY, Khaodeuanepheng NP, Amarasekara DL, Correia JJ, Lewis KA, Fitzkee NC, et al. Intrinsically disordered regions that drive phase separation form a robustly distinct protein class. J Biol Chem. 2023;299(1):102801.
83. Shapiro DM, Ney M, Eghtesadi SA, Chilkoti A. Protein Phase Separation Arising from Intrinsic Disorder: First-Principles to Bespoke Applications. J Phys Chem. 2021;125(25):6740–59.
84. Li J, Zhang M, Ma W, Yang B, Lu H, Zhou F, et al. Post-translational modifications in liquid-liquid phase separation: a comprehensive review. Mol Biomed. 2022;3(1):13.
85. Huang H, Sabari BR, Garcia BA, Allis CD, Zhao Y, SnapShot. Histone Modifications Cell. 2014;159(2):458–e1.
86. Zhao Y, Garcia BA. Comprehensive Catalog of Currently Documented Histone Modifications. Cold Spring Harb Perspect Biol. 2015;7(9):a025064.
87. Patel R, Loverde SM. Unveiling the Conformational Dynamics of the Histone Tails Using Markov State Modeling. J Chem Theory Comput. 2025;21(9):4921–38.
88. Wang X, Moore SC, Laszckzak M, Ausió J. Acetylation increases the alpha-helical content of the histone tails of the nucleosome. J Biol Chem. 2000;275(45):35013–20.
89. Hammonds EF, Singh A, Suresh KK, Yang S, Zahorodny SSM, Gupta R et al. Histone H3 tail charge patterns govern nucleosome condensate formation and dynamics. bioRxiv. 2025.
90. Stefansson OA, Sigurpalsdottir BD, Rognvaldsson S, Halldorsson GH, Juliusson K, Sveinbjornsson G, et al. The correlation between CpG methylation and gene expression is driven by sequence variants. Nat Genet. 2024;56(8):1624–31.
91. Wu SY, Lee CF, Lai HT, Yu CT, Lee JE, Zuo H, et al. Opposing Functions of BRD4 Isoforms in Breast Cancer. Mol Cell. 2020;78(6):1114–e3210.
92. Drumond-Bock AL, Wang L, Wang L, Cybula M, Rostworowska M, Kinter M, et al. Increased expression of BRD4 isoforms long (BRD4-L) and short (BRD4-S) promotes chemotherapy resistance in high-grade serous ovarian carcinoma. Genes Cancer. 2023;14:56–76.
93. Wu SY, Lai HT, Sanjib Banerjee N, Ma Z, Santana JF, Wei S, et al. IDR-targeting compounds suppress HPV genome replication via disruption of phospho-BRD4 association with DNA damage response factors. Mol Cell. 2024;84(2):202–20. e15.
94. Jung M, Philpott M, Muller S, Schulze J, Badock V, Eberspacher U, et al. Affinity map of bromodomain protein 4 (BRD4) interactions with the histone H4 tail and the small molecule inhibitor JQ1. J Biol Chem. 2014;289(13):9304–19.
95. Han X, Yu D, Gu R, Jia Y, Wang Q, Jaganathan A, et al. Roles of the BRD4 short isoform in phase separation and active gene transcription. Nat Struct Mol Biol. 2020;27(4):333–41.
96. Wang Y, Chen Y, Li M, Wang J, Jiang Y, Xie R et al. Phase separation of SPIN1 through its IDR facilitates histone methylation readout and tumorigenesis. J Mol Cell Biol. 2024;16(6).
97. Meehan RR, Lewis JD, Bird AP. Characterization of MeCP2, a vertebrate DNA binding protein with affinity for methylated DNA. Nucleic Acids Res. 1992;20(19):5085–92.
98. Liyanage V, Rastegar M. Rett syndrome and MeCP2. Neuromolecular Med. 2014;16(2):231–64.
99. Ishibashi T, Thambirajah AA, Ausio J. MeCP2 preferentially binds to methylated linker DNA in the absence of the terminal tail of histone H3 and independently of histone acetylation. FEBS Lett. 2008;582(7):1157–62.
100. Fraga MF, Ballestar E, Montoya G, Taysavang P, Wade PA, Esteller M. The affinity of different MBD proteins for a specific methylated locus depends on their intrinsic binding properties. Nucleic Acids Res. 2003;31(6):1765–74.
101. Moore JR, Nemera MT, D'Souza RD, Hamagami N, Clemens AW, Beard DC et al. MeCP2 and non-CG DNA methylation stabilize the expression of long genes that distinguish closely related neuron types. Nat Neurosci. 2025.
102. Ibrahim A, Papin C, Mohideen-Abdul K, Le Gras S, Stoll I, Bronner C, et al. MeCP2 is a microsatellite binding protein that protects CA repeats from nucleosome invasion. Volume 372. New York, NY: Science; 2021. p. 6549.
103. Thambirajah AA, Ng MK, Frehlick LJ, Li A, Serpa JJ, Petrotchenko EV, et al. MeCP2 binds to nucleosome free (linker DNA) regions and to H3K9/H3K27 methylated nucleosomes in the brain. Nucleic Acids Res. 2012;40(7):2884–97.

104. Padhan J, Sudhamalla B. Methyl-CpG Binding Protein 2 Reads Histone Methylation via an Aromatic Cage to Regulate Gene Expression and Chromatin Association. J Biol Chem. 2025:111115.
105. Ortega-Alarcon D, Claveria-Gimeno R, Vega S, Kalani L, Jorge-Torres OC, Esteller M, et al. Extending MeCP2 interactome: canonical nucleosomal histones interact with MeCP2. Nucleic Acids Res. 2024;52(7):3636–53.
106. Adams VH, McBryant SJ, Wade PA, Woodcock CL, Hansen JC. Intrinsic disorder and autonomous domain function in the multifunctional nuclear protein, MeCP2. J Biol Chem. 2007;282(20):15057–64.
107. Fan C, Zhang H, Fu L, Li Y, Du Y, Qiu Z, et al. Rett mutations attenuate phase separation of MeCP2. Cell Discov. 2020;6:38.
108. Wang L, Hu M, Zuo MQ, Zhao J, Wu D, Huang L et al. Rett syndrome-causing mutations compromise MeCP2-mediated liquid-liquid phase separation of chromatin. Cell Res. 2020.
109. Good K, Kalani L, Vincent J, Ausio J. Multifaceted roles of MeCP2 in cellular regulation and phase separation: implications for neurodevelopmental disorders, depression, and oxidative stress. Biochem Cell Biol. 2025;103:1–12.
110. Bellini E, Pavesi G, Barbiero I, Bergo A, Chandola C, Nawaz MS, et al. MeCP2 post-translational modifications: a mechanism to control its involvement in synaptic plasticity and homeostasis? Front Cell Neurosci. 2014;8:236.
111. Ausió J, de Paz A, Esteller M. MeCP2: the long trip from a chromatin protein to neurological disorders. Trends Mol Med. 2014;20(9):487–98.
112. Kalani L, Kim BH, Vincent JB, Ausio J. MeCP2 ubiquitination and sumoylation, in search of a functiondagger. Hum Mol Genet. 2023;33(1):1–11.
113. Li CH, Coffey EL, Dall'Agnese A, Hannett NM, Tang X, Henninger JE et al. MeCP2 links heterochromatin condensates and neurodevelopmental disease. Nature. 2020.
114. Zhang H, Romero H, Schmidt A, Gagova K, Qin W, Bertulat B, et al. MeCP2-induced heterochromatin organization is driven by oligomerization-based liquid-liquid phase separation and restricted by DNA methylation. Nucleus. 2022;13(1):1–34.
115. Reid XJ, Low JKK, Mackay JP. A NuRD for all seasons. Trends Biochem Sci. 2023;48(1):11–25.
116. Allen HF, Wade PA, Kutateladze TG. The NuRD architecture. Cell Mol Life Sci. 2013;70(19):3513–24.
117. Maurici N, Phan TM, Henty-Ridilla JL, Kim YC, Mittal J, Bah A. Uncovering the Molecular Interactions Underlying MBD2 and MBD3 Phase Separation. J Phys Chem. 2025;129(23):5728–43.
118. Tabar MS, Parsania C, Giardina C, Feng Y, Wong ACH, Metierre C, et al. Intrinsically Disordered Regions Define Unique Protein Interaction Networks in CHD Family Remodelers. FASEB J. 2025;39(10):e70632.
119. Flock T, Weatheritt RJ, Latysheva NS, Babu MM. Controlling entropy to tune the functions of intrinsically disordered regions. Curr Opin Struct Biol. 2014;26:62–72.
120. Moses D, Ginell GM, Holehouse AS, Sukenik S. Intrinsically disordered regions are poised to act as sensors of cellular chemistry. Trends Biochem Sci. 2023;48(12):1019–34.
121. James TC, Elgin SC. Identification of a nonhistone chromosomal protein associated with heterochromatin in Drosophila melanogaster and its gene. Mol Cell Biol. 1986;6(11):3862–72.
122. Eissenberg JC, James TC, Foster-Hartnett DM, Hartnett T, Ngan V, Elgin SC. Mutation in a heterochromatin-specific chromosomal protein is associated with suppression of position-effect variegation in Drosophila melanogaster. Proc Natl Acad Sci USA. 1990;87(24):9923–7.
123. Kwon SH, Workman JL. The heterochromatin protein 1 (HP1) family: put away a bias toward HP1. Mol Cells. 2008;26(3):217–27.
124. Hiragami K, Festenstein R. Heterochromatin protein 1: a pervasive controlling influence. Cell Mol Life Sci. 2005;62(23):2711–26.
125. Meyer-Nava S, Nieto-Caballero VE, Zurita M, Valadez-Graham V. Insights into HP1a-Chromatin Interactions. Cells. 2020;9(8).
126. Singh PB, Georgatos SD. HP1: facts, open questions, and speculation. J Struct Biol. 2002;140(1–3):10–6.
127. Bannister AJ, Zegerman P, Partridge JF, Miska EA, Thomas JO, Allshire RC, et al. Selective recognition of methylated lysine 9 on histone H3 by the HP1 chromo domain. Nature. 2001;410(6824):120–4.
128. Lachner M, O'Carroll D, Rea S, Mechtler K, Jenuwein T. Methylation of histone H3 lysine 9 creates a binding site for HP1 proteins. Nature. 2001;410(6824):116–20.
129. Nielsen PR, Nietlispach D, Mott HR, Callaghan J, Bannister A, Kouzarides T, et al. Structure of the HP1 chromodomain bound to histone H3 methylated at lysine 9. Nature. 2002;416(6876):103–7.
130. Gonzalez J, Bosch-Presegue L, Marazuela-Duque A, Guitart-Solanes A, Espinosa-Alcantud M, Fernandez AF, et al. A complex interplay between H2A.Z and HP1 isoforms regulates pericentric heterochromatin. Front Cell Dev Biol. 2023;11:1293122.
131. Fanti L, Pimpinelli S. HP1: a functionally multifaceted protein. Curr Opin Genet Dev. 2008;18(2):169–74.
132. Guthmann M, Burton A, Torres-Padilla ME. Expression and phase separation potential of heterochromatin proteins during early mouse development. EMBO Rep. 2019;20(12):e47952.
133. Eirin-Lopez JM, Ausio J. Origin and evolution of chromosomal sperm proteins. BioEssays. 2009;31(10):1062–70.
134. Alberti S, Gladfelter A, Mittag T. Considerations and Challenges in Studying Liquid-Liquid Phase Separation and Biomolecular Condensates. Cell. 2019;176(3):419–34.
135. Li LG, Hou Z. Theoretical modelling of liquid-liquid phase separation: from particle-based to field-based simulation. Biophys Rep. 2022;8(2):55–67.
136. Shin Y, Brangwynne CP. Liquid phase condensation in cell physiology and disease. Volume 357. New York, NY: Science; 2017. 6357.
137. Rippe K. Liquid-Liquid Phase Separation in Chromatin. Cold Spring Harb Perspect Biol. 2022;14(2).
138. Hansen JC, Maeshima K, Hendzel MJ. The solid and liquid states of chromatin. Epigenetics chromatin. 2021;14(1):50.
139. Golembeski A, Lequieu J. A Molecular View into the Structure and Dynamics of Phase-Separated Chromatin. J Phys Chem. 2024;128(43):10593–603.
140. Chen L, Maristany MJ, Farr SE, Luo J, Gibson BA, Doolittle LK, et al. Nucleosome spacing can fine-tune higher-order chromatin assembly. Nat Commun. 2025;16(1):6315.
141. Watson M, Sabirova D, Hardy MC, Pan Y, Carpentier DCJ, Yates H, et al. A DNA condensation code for linker histones. Proc Natl Acad Sci USA. 2024;121(33):e2409167121.
142. Kyu T, Ilies I, Shen C. Liquid-Crystalline Polymer Systems: Technological Advances. In: Isayev AI, Kyu T, Cheng SZD, editors. ACS Symposyum Series 632 ACS. Washington, D.C.: American Chemical Society; 1996. pp. 201–15.
143. Lin Z, Zhang H, Yang Y. Spinodal decomposition kinetics of a mixture of liquid crystals and polymers. Macromol Chem Phys. 1993;200:943–8.
144. Winkler A, Virnau P, Binder K, Winkler RG, Gompper G. Hydrodynamic mechanisms of spinodal decomposition in confined colloid-polymer mixtures: a multiparticle collision dynamics study. J Chem Phys. 2013;138(5):054901.
145. Reith D, Bucior K, Yelash L, Virnau P, Binder K. Spinodal decomposition of polymer solutions: molecular dynamics simulations of the two-dimensional case. J Phys Condens Matter. 2012;24(11):115102.
146. Harrison LG, Kasinsky HE, Ribes E, Chiva M. Possible mechanisms for early and intermediate stages of sperm chromatin condensation patterning involving phase separation dynamics. J Exp Zoolog Comp Exp Biol. 2005;303(1):76–92.
147. Ahlawat V, Kota HEM, Zhou D. Measuring bridging forces in protein–DNA condensates. Proc Natl Acad Sci USA. 2026;121(3):e2523058123.
148. Marcon L, Boissonneault G. Transient DNA strand breaks during mouse and human spermiogenesis new insights in stage specificity and link to chromatin remodeling. Biol Reprod. 2004;70(4):910–8.
149. Mukherjee A, de Izarra A, Degrouard J, Olive E, Maiti PK, Jang YH, et al. Protamine-Controlled Reversible DNA Packaging: A Molecular Glue. ACS Nano. 2021;15(8):13094–104.
150. Cremer T, Cremer M, Hubner B, Silahtaroglu A, Hendzel M, Lanctot C, et al. The Interchromatin Compartment Participates in the Structural and Functional Organization of the Cell Nucleus. BioEssays. 2020;42(2):e1900132.
151. Chiva M, Saperas N, Ribes E. Complex chromatin condensation patterns and nuclear protein transitions during spermiogenesis: examples from mollusks. Tissue Cell. 2011;43(6):367–76.
152. Kasinsky HE, Ellis S, Martens G, Ausio J. Dynamic aspects of spermiogenic chromatin condensation patterning by phase separation during the histone-to-protamine transition in charalean algae and relation to bryophytes. Tissue Cell. 2014;46(6):415–32.
153. Kasinsky HE, Gowen BE, Ausio J. Spermiogenic chromatin condensation patterning in several hexapods may involve phase separation dynamics by spinodal decomposition or microemulsion inversion (nucleation). Tissue Cell. 2021;73:101648.
154. Gusse M, Chevaillier P. [Ultrastructural and chemical study of the chromatin during spermiogenesis of the fish Scyliorhinus caniculus (L.) (author's transl)]. Cytobiologie. 1978;16(3):421–43.
155. Herraez MP, Ausió J, Devaux A, Gonzalez-Rojo S, Fernandez-Diez C, Bony S, et al. Paternal contribution to development. Sperm genetic damage and repair in fish. Aquaculture. 2017;472:45–59.

156. Ausio J, Gonzalez-Romero R, Woodcock CL. Comparative structure of vertebrate sperm chromatin. J Struct Biol. 2014;188(2):142–55.
157. Lewis JD, Song Y, de Jong ME, Bagha SM, Ausio J. A walk though vertebrate and invertebrate protamines. Chromosoma. 2003;111(8):473–82.
158. Vivante A, Bronshtein I, Garini Y. Chromatin Viscoelasticity Measured by Local Dynamic Analysis. Biophys J. 2020;118(9):2258–67.
159. Subirana JA. Order and disorder in 30 nm chromatin fibers. FEBS Lett. 1992;302(2):105–7.
160. Gibson BA, Blaukopf C, Lou T, Chen L, Doolittle LK, Finkelstein I, et al. In diverse conditions, intrinsic chromatin condensates have liquid-like material properties. Proc Natl Acad Sci USA. 2023;120(18):e2218085120.
161. Gibson BA, Doolittle LK, Schneider MWG, Jensen LE, Gamarra N, Henry L, et al. Organization of Chromatin by Intrinsic and Regulated Phase Separation. Cell. 2019;179(2):470–84. e21.
162. Strickfaden H, Tolsma TO, Sharma A, Underhill DA, Hansen JC, Hendzel MJ. Condensed Chromatin Behaves like a Solid on the Mesoscale In Vitro and in Living Cells. Cell. 2020;183(7):1772–e8413.
163. Muzzopappa F, Hertzog M, Erdel F. DNA length tunes the fluidity of DNA-based condensates. Biophys J. 2021;120(7):1288–300.
164. Zhou H, Huertas J, Maristany MJ, Russell K, Hwang JH, Yao RW, et al. Multiscale structure of chromatin condensates explains phase separation and material properties. Volume 390. New York, NY: Science; 2025. p. eadv6588. 6777.
165. Ridsdale JA, Hendzel MJ, Delcuve GP, Davie JR. Histone acetylation alters the capacity of the H1 histones to condense transcriptionally active/competent chromatin. J Biol Chem. 1990;265(9):5150–6.
166. Garcia-Ramirez M, Rocchini C, Ausio J. Modulation of chromatin folding by histone acetylation. J Biol Chem. 1995;270(30):17923–8.
167. Erdel F, Rippe K. Formation of Chromatin Subcompartments by Phase Separation. Biophys J. 2018;114(10):2262–70.
168. Siqueira E, Kim BH, Reser L, Chow R, Delaney K, Esteller M, et al. Analysis of the interplay between MeCP2 and histone H1 during in vitro differentiation of human ReNCell neural progenitor cells. Epigenetics. 2023;18(1):2276425.
169. Serna-Pujol N, Salinas-Pena M, Mugianesi F, Le Dily F, Marti-Renom MA, Jordan A. Coordinated changes in gene expression, H1 variant distribution and genome 3D conformation in response to H1 depletion. Nucleic Acids Res. 2022.
170. Hales TC, Sarnak P, Pugh MC. Advances in random matrix theory, zeta functions, and sphere packing. Proc Natl Acad Sci USA. 2000;97(24):12963–4.
171. Dixon JR, Selvaraj S, Yue F, Kim A, Li Y, Shen Y, et al. Topological domains in mammalian genomes identified by analysis of chromatin interactions. Nature. 2012;485(7398):376–80.
172. Szabo Q, Donjon A, Jerkovic I, Papadopoulos GL, Cheutin T, Bonev B, et al. Regulation of single-cell genome organization into TADs and chromatin nanodomains. Nat Genet. 2020;52(11):1151–7.
173. Zhao JZ, Xia J, Brangwynne CP. Mechanical regulation and activity of nuclear condensates. Biophys J. 2025.
174. Fawcett DW, Anderson WA, Phillips DM. Morphogenetic factors influencing the shape of the sperm head. Dev Biol. 1971;26(2):220–51.
175. Czernik M, Palazzese L, Winiarczyk D, Iuso D, Khochbin S, Fulka J, et al. Protamine sequence determines species-specific nuclear shape and histone retention. iScience. 2025;28(8):113102.
176. Uversky VN. A blurry view of fuzzy objects: on the roles of low-resolution structural techniques in discoveryand early characterization of intrinsically disordered proteins. Frontiers in Biophysics; 2025.
177. Park S, Merino-Urteaga R, Karwacki-Neisius V, Carrizo GE, Athreya A, Marin-Gonzalez A, et al. Native nucleosomes intrinsically encode genome organization principles. Nature. 2025;643(8071):572–81.
178. Rippe K, Papantonis A. RNA polymerase II transcription compartments - from factories to condensates. Nat Rev. 2025;26(11):775–88.
179. Demmerle J, Hao S, Cai D. Transcriptional condensates and phase separation: condensing information across scales and mechanisms. Nucleus. 2023;14(1):2213551.
180. Benabdallah NS, Williamson I, Illingworth RS, Kane L, Boyle S, Sengupta D, et al. Decreased Enhancer-Promoter Proximity Accompanying Enhancer Activation. Mol Cell. 2019;76(3):473–84. e7.
181. Henninger JE, Oksuz O, Shrinivas K, Sagi I, LeRoy G, Zheng MM, et al. RNA-Mediated Feedback Control Transcriptional Condensates Cell. 2021;184(1):207–25. e24.
182. Quinodoz SA, Jachowicz JW, Bhat P, Ollikainen N, Banerjee AK, Goronzy IN, et al. RNA promotes the formation of spatial compartments in the nucleus. Cell. 2021;184(23):5775–e9030.
183. Dorighi KM, Swigut T, Henriques T, Bhanu NV, Scruggs BS, Nady N, et al. Mll3 and Mll4 Facilitate Enhancer RNA Synthesis and Transcription from Promoters Independently of H3K4 Monomethylation. Mol Cell. 2017;66(4):568–e764.
184. Shahib AK, Rastegar M, van Wijnen AJ, Davie JR. Neurodevelopmental functions and activities of the KAT3 class of lysine acetyltransferases. Biochem Cell Biol. 2024;102(6):430–47.
185. Ma L, Gao Z, Wu J, Zhong B, Xie Y, Huang W, et al. Co-condensation between transcription factor and coactivator p300 modulates transcriptional bursting kinetics. Mol Cell. 2021;81(8):1682–97. e7.
186. Sabari BR, Dall'Agnese A, Boija A, Klein IA, Coffey EL, Shrinivas K, et al. Coactivator condensation at super-enhancers links phase separation and gene control. Sci (New York NY). 2018;19:eaar3958–17.
187. Ferrie JJ, Karr JP, Tjian R, Darzacq X. Structure-function relationships in eukaryotic transcription factors: The role of intrinsically disordered regions in gene regulation. Mol Cell. 2022;82(21):3970–84.
188. Devaiah BN, Singh AK, Mu J, Chen Q, Meerzaman D, Singer DS. Phosphorylation by JNK switches BRD4 functions. Mol Cell. 2024;84(22):4282–e967.
189. Zhang Q, Shi H, Zhang Z. Dynamic kissing model for enhancer-promoter communication on the surface of transcriptional condensates. Phys Rev E. 2025;111(5–1):054402.
190. Du M, Stitzinger SH, Spille JH, Cho WK, Lee C, Hijaz M, et al. Direct observation of a condensate effect on super-enhancer controlled gene bursting. Cell. 2024;187(2):331–44. e17.
191. Geisler MS, Kemp JP Jr., Duronio RJ. Histone locus bodies: a paradigm for how nuclear biomolecular condensates control cell cycle regulated gene expression. Nucleus. 2023;14(1):2293604.
192. Xu SB, Gao XK, Liang HD, Cong XX, Chen XQ, Zou WK et al. KPNA3 regulates histone locus body formation by modulating condensation and nuclear import of NPAT. J Cell Biol. 2025;224(1).
193. Osborne CS, Chakalova L, Brown KE, Carter D, Horton A, Debrand E, et al. Active genes dynamically colocalize to shared sites of ongoing transcription. Nat Genet. 2004;36(10):1065–71.
194. Jackson DA, Hassan AB, Errington RJ, Cook PR. Visualization of focal sites of transcription within human nuclei. EMBO J. 1993;12(3):1059–65.
195. Jackson DA. Chromatin domains and nuclear compartments: establishing sites of gene expression in eukaryotic nuclei. Mol Biol Rep. 1997;24(3):209–20.
196. Jackson DA, Cook PR. Transcription occurs at a nucleoskeleton. EMBO J. 1985;4(4):919–25.
197. Jackson DA, Cook PR. The structural basis of nuclear function. Int Rev Cytol. 1995;162A:125–49.
198. Ma G, Fu X, Zhou L, Babarinde IA, Shi L, Yang W, et al. The nuclear matrix stabilizes primed-specific genes in human pluripotent stem cells. Nat Cell Biol. 2025;27(2):232–45.
199. Hendzel MJ, Sun JM, Chen HY, Rattner JB, Davie JR. Histone acetyltransferase is associated with the nuclear matrix. J Biol Chem. 1994;269(36):22894–901.
200. Aoi Y, Shilatifard A. Transcriptional elongation control in developmental gene expression, aging, and disease. Mol Cell. 2023;83(22):3972–99.
201. Guo C, Zhang Y, Shuai S, Sigbessia A, Hao S, Xie P, et al. The super elongation complex (SEC) mediates phase transition of SPT5 during transcriptional pause release. EMBO Rep. 2023;24(3):e55699.
202. Sun R, Fisher RP. The CDK9-SPT5 Axis in Control of Transcription Elongation by RNAPII. J Mol Biol. 2025;437(1):168746.
203. Rawat P, Sawarkar R. SPTing across condensates: SEC-mediated translocation of SPT complex from pausing condensates to elongation condensates. EMBO Rep. 2023;24(3):e56810.
204. Aoki D, Awazu A, Fujii M, Uewaki JI, Hashimoto M, Tochio N, et al. Ultrasensitive Change in Nucleosome Binding by Multiple Phosphorylations to the Intrinsically Disordered Region of the Histone Chaperone FACT. J Mol Biol. 2020;432(16):4637–57.
205. Shakya A, Park S, Rana N, King JT. Liquid-Liquid Phase Separation of Histone Proteins in Cells: Role in Chromatin Organization. Biophys J. 2020;118(3):753–64.
206. Keenen MM, Brown D, Brennan LD, Renger R, Khoo H, Carlson CR et al. HP1 proteins compact DNA into mechanically and positionally stable phase separated domains. eLife. 2021;10.
207. Furukawa A, Yonezawa K, Negami T, Yoshimura Y, Hayashi A, Nakayama JI et al. A dynamic structural unit of phase-separated heterochromatin protein 1alpha as revealed by integrative structural analyses. Nucleic Acids Res. 2025;53(6).
208. Strom AR, Emelyanov AV, Mir M, Fyodorov DV, Darzacq X, Karpen GH. Phase separation drives heterochromatin domain formation. Nature. 2017;547(7662):241–5.

209. Larson AG, Elnatan D, Keenen MM, Trnka MJ, Johnston JB, Burlingame AL, et al. Liquid droplet formation by HP1alpha suggests a role for phase separation in heterochromatin. Nature. 2017;547(7662):236–40.
210. Her C, Phan TM, Jovic N, Kapoor U, Ackermann BE, Rizuan A, et al. Molecular interactions underlying the phase separation of HP1alpha: role of phosphorylation, ligand and nucleic acid binding. Nucleic Acids Res. 2022;50(22):12702–22.
211. Zhai Z, Soman A, Kuang J, Guo J, Chen Y, Zhao L, et al. Revealing site-specific molecular features mediating contacts of heterochromatin protein 1 alpha (HP1alpha) and the interactions with chromatin and DNA in LLPS environments. Commun Biol. 2025;8(1):1758.
212. Bohra D, Mazumder A. HP1 isoforms direct repair pathway choice in response to heterochromatin double-strand breaks. J Cell Biol. 2026;225(3).
213. Erdel F, Rademacher A, Vlijm R, Tunnermann J, Frank L, Weinmann R, et al. Mouse Heterochromatin Adopts Digital Compaction States without Showing Hallmarks of HP1-Driven Liquid-Liquid Phase Separation. Mol Cell. 2020;78(2):236–49. e7.
214. Gitler AD, Shorter J, Ha T, Myong S. Just Took a DNA Test, Turns Out 100% Not That Phase. Mol Cell. 2020;78(2):193–4.
215. Feric M, Misteli T. Phase separation in genome organization across evolution. Trends Cell Biol. 2021;31(8):671–85.
216. Bensaha S, Lewandowska D, Muzzopappa F, Hutin S, Tully MD, Anfossi M, et al. HP1 loses its chromatin clustering and phase separation function across evolution. Nat Commun. 2025;16(1):6375.
217. Phan TM, Kim YC, Debelouchina GT, Mittal J. Interplay between charge distribution and DNA in shaping HP1 paralog phase separation and localization. eLife. 2024;12.
218. Calinsky R, Levy Y. A pH-Dependent Coarse-Grained Model for Disordered Proteins: Histidine Interactions Modulate Conformational Ensembles. J Phys Chem Lett. 2024;15(37):9419–30.
219. Guillen-Chable F, Bayona A, Rodriguez-Zapata LC, Castano E. Phase Separation of Intrinsically Disordered Nucleolar Proteins Relate to Localization and Function. Int J Mol Sci. 2021;22(23).
220. Mitrea DM, Cika JA, Stanley CB, Nourse A, Onuchic PL, Banerjee PR, et al. Self-interaction of NPM1 modulates multiple mechanisms of liquid-liquid phase separation. Nat Commun. 2018;9(1):842.
221. Zhang X, Li W, Sun S, Liu Y. Advances in the structure and function of the nucleolar protein fibrillarin. Front Cell Dev Biol. 2024;12:1494631.
222. Tonello F, Massimino ML, Peggion C. Nucleolin: a cell portal for viruses, bacteria, and toxins. Cell Mol Life Sci. 2022;79(5):271.
223. Spaulding EL, Feidler AM, Cook LA, Updike DL. RG/RGG repeats in the C. elegans homologs of Nucleolin and GAR1 contribute to sub-nucleolar phase separation. Nat Commun. 2022;13(1):6585.
224. Mao YS, Zhang B, Spector DL. Biogenesis and function of nuclear bodies. Trends Genet. 2011;27(8):295–306.
225. Dekker J, Oksuz BA, Zhang Y, Wang Y, Minsk MK, Kuang S et al. An integrated view of the structure and function of the human 4D nucleome. Nature. 2025.
226. Choi S, Lee JM, Kim KK. Biomolecular condensates: molecular structure, biological functions, diseases, and therapeutic targets. Mol Biomed. 2025;6(1):99.
227. Saitoh N, Spahr CS, Patterson SD, Bubulya P, Neuwald AF, Spector DL. Proteomic analysis of interchromatin granule clusters. Mol Biol Cell. 2004;15(8):3876–90.
228. Zhang M, Gu Z, Guo S, Sun Y, Ma S, Yang S, et al. SRRM2 phase separation drives assembly of nuclear speckle subcompartments. Cell Rep. 2024;43(3):113827.
229. Grau LP, Azorin F, Subirana JA. Aggregation of mono- and dinucleosomes into chromatin-like fibers. Chromosoma. 1982;87(4):437–45.
230. Maeshima K, Rogge R, Tamura S, Joti Y, Hikima T, Szerlong H, et al. Nucleosomal arrays self-assemble into supramolecular globular structures lacking 30-nm fibers. EMBO J. 2016;35(10):1115–32.
231. Garcia Ramirez M, Dong F, Ausió J. Role of the histone tails in the folding of oligonucleosomes depleted of histone H1. J Biol Chem. 1992;267(27):19587–95.

Publisher's Note